

Addressing zero-inflated and mis-measured functional predictors in scalar-on-function regression model

Heyang Ji¹, Lan Xue², Ufuk Beyaztas³, Roger S. Zoh¹, Jeff Goldsmith⁴, Mark Benden⁵, and Carmen D. Tekwe¹

¹Department of Epidemiology and Biostatistics, Indiana University School of Public Health, Bloomington, Indiana, USA

²Department of Statistics, Oregon State University College of Science, Corvallis, Oregon, USA

³Department of Statistics, Marmara University Faculty of Sciences , Istanbul, Turkiye

⁴Department of Biostatistics, Columbia University Mailman School of Public Health, New York, New York, USA

⁵Department of Environmental & Occupational Health, Texas A&M University School of Public Health, College Station, Texas, USA

Abstract

Wearable devices are often used in clinical and epidemiological studies to monitor physical activity behavior and its influence on health outcomes. These devices are worn over multiple days to record activity patterns, such as step counts recorded at the minute level, resulting in multi-level, longitudinal, high-dimensional, or functional data. When monitoring patterns of step counts over multiple days, devices may record excess zeros during periods of sedentary behavior or non-wear times. Additionally, it has been demonstrated that the accuracy of wearable devices in monitoring true physical activity patterns depends on the intensity of the activities and wear times. While work on adjusting for biases due to measurement errors in functional data is a growing field, relatively less work has been done to study the occurrence of excess zeros along with measurement errors and their combined influence on estimation and inference in multi-level scalar-on-function regression models. We propose semi-continuous modeling approaches to adjust for biases due to zero inflation and measurement errors in scalar-on-function regression models. We provide theoretical justifications for our proposed methods and, through extensive simulations, we demonstrated their finite sample properties. Finally, the developed methods are applied to a school-based intervention study examining the association between school day physical activity with age- and sex-adjusted body mass index among elementary school-aged children.

1 Introduction

With the rapid advancement of digital health technologies (Friend et al., 2023), wearable devices have increasingly been used for continuous monitoring and collection of biobehavioral data. Examples include physical activity (Teixeira et al., 2021; Coughlin and Stewart, 2016; Strain et al., 2020; Wang et al., 2022; Phillips et al., 2018), blood glucose levels (Rodbard, 2016; Klonoff, 2005; Mastrototaro, 2000; Klonoff et al., 2017; Group, 2008), sleep (De Zambotti et al., 2019; Muaremi et al., 2013; Scott et al., 2020; Tobin et al., 2021; Sargent et al., 2018), and ambulatory blood pressure monitoring

(Pickering et al., 2006; O'Brien et al., 2018; Turner et al., 2015; Huang et al., 2021; Pickering, 1996). These measures are subsequently employed in epidemiological studies to evaluate their impact on health outcomes (McDonough et al., 2021; Phillips et al., 2018; Huang et al., 2021). Physical activity data gathered from Actigraph devices is an illustrative example(Troiano, 2023).

The ActiGraph GTx3+, utilized in the National Health and Nutrition Examination Survey (NHANES), is a wearable device that captures participants' triaxial data on device acceleration at sampling frequencies from 30Hz to 100Hz (Centers for Disease Control and Prevention, National Center for Health Statistics, 2020), with activity summaries like step counts reported in epochs with a duration of 60 seconds (ActiGraph, 2013). Wearable devices typically use shorter epoch durations to improve the accuracy of estimating intervals of intense physical activity (Ayabe et al., 2013). Shortened epochs are beneficial for real-time tracking, while extended epochs may distort brief yet critical fluctuations. For instance, intense exercise conducted over a few minutes, when recorded with a protracted epoch (such as one hour), might lead to only a slight increase in the average heart rate, failing to accurately depict the actual exertion period. These continuously gathered data, collected multiple times per hour over several days, produce multi-level, high-dimensional or functional datasets with intricate error configurations and patterns and functional data analysis is commonly used to analyze such datasets. (Ramsay et al., 2009).

Functional data analysis is a statistical approach frequently used to analyze high-dimensional data that appear as functions or images (Gertheiss et al., 2024; Wang et al., 2016). When a variable is densely sampled across time or space within a certain domain, it can be treated as a function and is usually assumed to be square-integrable (Bosq, 2000; Ramsay et al., 2009). Conventionally, densely collected data are designated as functional data, in contrast with sparsely sampled data, which may be described as longitudinal data depending on the context and modeling strategy (Wang et al., 2016). As noted, continuous monitoring yields high-dimensional data where one or more variables are measured at numerous time points. This leads to correlations among measurements from the same subject at different times, often with a complex structure and a resulting joint distribution that is challenging to model. Capturing such complexity typically requires statistical models with a large number of parameters, i.e., high degrees of freedom. One effective strategy to address this issue is to represent the data as realizations of functions, leveraging the flexibility of infinite-dimensional function spaces such as the L^2 space (Ferraty and Vieu, 2006). Functional data analysis provides a principled framework for analyzing such data, where high-dimensional observations are treated as smooth functions over time or space. In practice, these functions are approximated by linear combinations of a finite set of basis functions (Morris, 2015; Ramsay and Silverman, 2005). These functional representations can then be incorporated into regression frameworks, including generalized functional linear models, to explore associations between functional predictors and health outcomes.

Generalized linear regression models with scalar responses and predictors have been extended to generalized functional linear regression models, where predictors can be either functional or scalar, and responses may similarly be scalar or functional (Müller and Stadtmüller, 2005; Reiss et al., 2017). In these models, truncated complete basis such as the Fourier basis, functional principal components from the L^2 space, or linearly independent functions like B-splines are used to approximate the functional components (Reiss et al., 2017; Crainiceanu et al., 2024). In classical linear regression, the effect of each scalar predictor is represented by a scalar coefficient; in contrast, functional regression represents the effect of a functional predictor by a functional coefficient. To incorporate functional predictor into a linear model, the inner product in the L^2 space between the parameter function and the predictor function is used in place of the product of a scalar coefficient and a scalar predictor.

Monitoring behavioral patterns such as physical activity can lead to observations that are susceptible to measurement error (Rothney et al., 2008; Jeffries et al., 2014; Kozey et al., 2010). In functional data, observed values are often contaminated by random noise (i.e., measurement error) (Wang et al., 2016). Measurement error contamination in functional data has been widely recognized in the literature (Yao et al., 2005; Hall et al., 2006) (Bunn et al., 2018; Feehan et al., 2018; Atkinson and Nevill, 1998; Bassett Jr et al., 2012; Ferrari et al., 2007). Multiple sources contribute to measurement

error in physical activity data monitored by accelerometers. By definition, physical activity is bodily movement produced by skeletal muscles that results in energy expenditure (Caspersen et al., 1985; World Health Organization, 2019). Thus, data collected by wearable devices represent an estimation of physical activity based on detected movements. Various factors including monitor placement, individual characteristics (e.g., body weight), suboptimal dynamic range and sampling frequency, external disturbances (e.g., vehicular accelerations), activity type (e.g., walking, cycling, weight lifting), and differences in proprietary algorithms can affect the data output and introduce measurement error (Plasqui et al., 2013; Plasqui and Westerterp, 2007; Butte et al., 2012; Robertson et al., 2011; Corder et al., 2007; Rowlands et al., 2004).

Measurement errors may occur due to unobserved or unrecorded values or inaccuracies in measurement. Typically, in many studies, these errors are treated as independent both between and within individuals, often incorporated as an additive error term in regression models (Carroll et al., 1995; Fuller, 2009). Even when these errors have zero expectations, they can still introduce bias into parameter estimates. Naive averaging or smoothing approaches often fail to fully correct such bias and introduce attenuation in the estimated the effect of the error-prone variable. Therefore, more sophisticated methods are required to appropriately account for measurement error. Various functional data analysis methods have been developed to address measurement error (Crambes et al., 2009; Zhang et al., 2023; Tekwe et al., 2022), each tailored to specific assumptions about the error characteristics. For instance, some methods presuppose the errors are additive, independent of the true value, and exhibit short-range temporal correlation (Cardot et al., 2013). In certain scenarios, bias arising from measurement error is corrected by conceptualizing the error as an additive stationary Gaussian process with a zero mean, akin to white noise, on top of the genuine signal (Hall and Hosseini-Nasab, 2006). A variety of methods have been developed to address measurement error in functional data, including smoothing-based techniques (Ullah and Finch, 2013; Cardot et al., 2013; Florens and Van Bellegem, 2015) and instrumental variable approaches (Tekwe et al., 2022; Jadhav et al., 2022; Zoh et al., 2024), each relying on different assumptions about the nature of the error. However, not all measurement errors can be accurately characterized as white noise or similar simple zero-mean additive noise. Functional data may exhibit even more complex error structures. For example, measurement error problem can mix with zero inflation problem where the measurement errors are not additive to the true values, instead, the observed values are generated via a zero-inflated surrogate or observed measures. Zero inflation indicates an unexpectedly high frequency of zero values in the dataset (Lambert, 1992; Ridout et al., 1998; Tu, 2006). In count data, this means that zeros occur more frequently than predicted by standard models (e.g., Poisson or negative binomial) (Tait et al., 2012; Campbell, 2021; Shao et al., 2025). Continuous data can also be zero-inflated, often leading to violations of model assumptions and computational difficulties (Tu, 2006). In some cases, zero values correspond to missing data, while in others they represent true zeros. For example, when wearable devices record zero activity during periods of inactivity or sedentary behavior (Jeffries et al., 2014; Troiano et al., 2008; Matthews et al., 2008). To address excess zeros—particularly in scalar or non-functional data—researchers commonly employ mixture or semicontinuous models (Lee et al., 2010; Wang et al., 2024; Li et al., 2005; Mills, 2013; Tooze et al., 2002).

While numerous methods have been developed to address bias from measurement error in zero-inflated scalar data (Li et al., 2005; Mills, 2013; Tooze et al., 2002; Wang et al., 2024), much less work has been done in the context of functional data. In particular, methods that simultaneously account for both zero inflation and measurement error in functional predictors remain scarce. In this manuscript, we propose a mixture model to handle zero-inflated functional data with measurement error and develop parameter estimation methods that correct for the bias introduced by such errors. We demonstrate the robustness of our approach through simulation studies. The proposed method can extract meaningful insights from complex health and behavioral datasets. We apply our methods to data collected from children in a Texas school district to assess the relationships that school-based physical activity have with age- and sex- adjusted BMI. This dataset serves as a valuable real-world case study for evaluating how our method can uncover hidden patterns, assess intervention outcomes,

and improve predictive modeling in health-related educational research.

This manuscript is structured as follows. Section 2 introduces a multi-level generalized functional scalar-on-function regression model capable of handling zero-inflated functional predictors with measurement errors. Here, we detail the statistical model, the assumptions, estimation techniques, and the theoretical aspects of our approach. Section 3 describes a simulation study designed to assess our method's effectiveness compared to other methods. Section 4 demonstrates the application of our approach using data from obtained from elementary school-aged children from a Texas school district, examining the link between physical activity and body mass index (BMI) changes, adjusting for relevant demographics. Finally, section 5 highlights our key findings, while the discussion explores potential improvements and future directions for extending the methodology to address similar challenges.

2 Generalized scalar-on-function regression model with zero inflated functional predictors prone to measurement errors

We now define our proposed model along with the relevant assumptions. Let $\{Y_i, X_i(t), Z_i\}$ denote the data tuple for individual i ($i = 1, \dots, n$), where, Y_i is a scalar-valued response, $X_i(t) \in L^2(\Omega)$ is a functional predictor defined for $t \in \Omega$, and $Z_i \in \mathbb{R}^p$ is a vector of scalar predictors, with each element representing a distinct predictor. The functional variable $X_i(t)$ is latent and is observed indirectly via replicate measurements $W_{ij}(t)$ for $j = 1, \dots, J_i$. Here, Y_i represents a health outcome, $W_{ij}(t)$ represents the observed physical activity variable, $X_i(t)$ is the long-term expectation of $W_{ij}(t)$, and Z_i includes additional subject-level covariates such as age and sex. We propose the following models that frame the relationship of these variables:

$$Y_i \sim \text{EF}(\mu_i, \phi),$$

$$\mu_i = \mathbb{E}\{Y_i | X_i(t), Z_i\} = g^{-1} \left\{ \int_{\Omega} \beta(t) X_i(t) dt + (1, Z_i^\top) \gamma \right\}, \quad (1)$$

$$W_{ij}(t) = I\left[G_{ij}(t) < \Phi^{-1}\{p_i(t)\}\right] \cdot \left\{ \frac{X_i(t)}{p_i(t)} + U_{ij}(t) \right\}, \quad (2)$$

where μ_i denotes the conditional mean of Y_i given $X_i(t)$ and Z_i , $g(\cdot)$ is a strictly monotonic link function, $p_i(t)$ satisfies $p_i(t) \in (0, 1)$ for all i , Y_i follows a distribution from the exponential family, with density function of the form $f(y_i; \theta_i, \phi) = \exp \left\{ \frac{y_i \theta_i - b(\theta_i)}{a(\phi)} + c(y_i, \phi) \right\}$, θ_i is the canonical parameter, $\mu_i = b^\top(\theta_i)$ is the mean, ϕ is the dispersion parameter, and $a(\cdot)$, $b(\cdot)$, and $c(\cdot, \cdot)$ are known functions. We use the notation $Y_i \sim \text{EF}(\mu_i, \phi)$ as a shorthand for this family. The $p_i(t)$ serves as a activation probability, representing the probability of $W_{ij}(t) \neq 0$, and $\beta(t) \in L^2(\Omega)$ is the coefficient function associated with $X_i(t)$. The scaling of $X_i(t)$ by the activation probability $p_i(t)$ in Model (2) is a key feature of our model, as it ensures that the observed proxy $W_{ij}(t)$ is an unbiased measurement of the true latent function $X_i(t)$ in expectation. For the outcome distribution, when Y_i is continuous we assume a Gaussian distribution as EF and adopt the identity link, i.e., $g(\mu) = \mu$. For binary outcomes, we assume a Bernoulli distribution as EF and use the logit link, i.e., $g(\mu) = \ln \left(\frac{\mu}{1-\mu} \right)$. In contrast, Y_i and Z_i are assumed to be measured without error. Finally, $\{G_{ij}(t), t \in \Omega\}$ and $\{U_{ij}(t), t \in \Omega\}$ are assumed to be latent, independent Gaussian processes.

2.1 Model assumptions

Our objective is to estimate the parameters $\beta(t)$ and γ in Model (1). Prior to estimation, to ensure that the proposed model adequately reflects the underlying data structure and supports valid statistical inference, we impose a set of assumptions. These assumptions provide realistic distributional conditions for the observed variables and are intended to facilitate the identifiability and estimability of model parameters.

- (A1) For $G_{ij}(t)$, we have $\mathbb{E}\{G_{ij}(t)\} = 0$ and $\text{Var}\{G_{ij}(t)\} = 1$, for all $t \in \Omega$ and i, j . $G_{ij}(t)$ are independent across individual index i but can be correlated across replication index j . $G_{ij}(t)$ have unspecified correlation structure across t . $G_{ij}(t)$ is independent to $X_i(t)$ and $U_{ij}(t)$.
- (A2) $\mathbb{E}\{U_{ij}(t)\} = 0$ for all $t \in \Omega$ and $\text{Var}\{U_{ij}(t)\} = \sigma_u^2(t)$. $U_{ij}(t)$ have unspecified correlation structure across t .
- (A3) The predictor process $\{X_i(t), t \in \Omega\}$ is Gaussian with $\mathbb{E}\{X_i(t)\} = \mu_x(t)$ and $\text{Var}\{X_i(t)\} = \sigma_x^2(t)$. $X_i(t)$ have unspecified correlation structure across t .
- (A4) For $p_i(t)$, we assume it is determined by the following model:

$$\text{logit}\{p_i(t)\} = (1, Z_i^\top) \theta(t). \quad (3)$$

Assumption (A1) ensures that the binary term $I[G_{ij}(t) < \Phi^{-1}\{p_i(t)\}]$ follows distribution $\text{Be}\{p_i(t)\}$ for each i and t , where Be stands for the Bernoulli distribution. The term $p_i(t)$ represents the probability of activation for individual i at time t . Assumption (A1) represents a relaxation of the stronger condition that $\{G_{ij}(t), t \in \Omega\}$ are independent across individuals and measurement occasions. While our methods are designed to work when this independence condition is met, they are also applicable to certain exceptions to this independence assumption. Assumptions (A2)-(A3) establish that for non-zero values, $W_{ij}(t)$ should have an expected value equating to $X_i(t)/p_i(t)$. Consequently, according to assumption (A1), $\mathbb{E}[W_{ij}(t)] = X_i(t)$. We impose assumption (A4) due to noticeable variations in the proportion of zero readings in physical activity data among different groups (e.g., varying age groups) (Nobre et al., 2017). These observations suggest that the probability of observing a nonzero activity level, $\Pr\{W_{ij}(t) \neq 0\} = p_i(t)$, may not be constant across individuals. Instead, it may depend on subject-specific characteristics such as age, sex, or socioeconomic status. Therefore, we model the log-odds of a nonzero observation using a time-varying coefficient model, where scalar predictors Z_i are allowed to influence $p_i(t)$ through the function $\theta(t)$.

2.2 Predicting the unobserved predictor

With the model and necessary assumptions in place, we now proceed to the estimation of the model parameters. The goal is to develop an estimation procedure that leverages the structure of the model while respecting the imposed assumptions. In an ideal scenario where all predictors in Model (1) are fully observed, one could directly extend methods for solving scalar-on-scalar regression model to scalar-on-function regression model using basis expansion. However, the functional predictor, $X_i(t)$, is latent and is only observed indirectly through its proxy, $W_{ij}(t)$. This leads to a model with multiple high-dimensional latent variables, resulting in a likelihood function with complex integrals and treating $X_i(t)$ as a parameter making the maximum likelihood estimation computationally intensive. A practical alternative is to substitute $X_i(t)$ with a predictor $\hat{X}_i(t)$ constructed from the observed measures or proxies, $W_{ij}(t)$. One important challenge is that measurements from the same individual at different values of t may be correlated. Jointly predicting $X_i(t)$ across all

time points would require specifying the full joint distribution of $X_i(t)$ and $W_{ij}(t)$, which involves assumptions about time-based correlation structures. If these assumptions do not accurately reflect the true process, the prediction may be adversely affected. On the other hand, predicting $X_i(t)$ independently at each time point avoids the need for these correlation structure assumptions and can significantly reduce the computational load. A naive approach would be to use the sample mean, $\bar{W}_{i\cdot}(t) = \frac{1}{J_i} \sum_{j=1}^{J_i} W_{ij}(t)$, exploiting the property $\mathbb{E}\{W_{ij}(t)\} = X_i(t)$. However, when plugging this estimator as the substitution of $X_i(t)$ in to the Model (1), it does not fully leverage the information contained in $W_{ij}(t)$ and may result in both bias and inefficiency. Alternatively, one might use a single observation (e.g., $\hat{X}_i(t) = W_{i1}(t)$, the measurement from the first day), but this approach is similarly suboptimal. In this article, to predict the latent predictor $X_i(t)$, we propose two distinct but related pointwise strategies. The first leverages a mixed-effects model representation of the non-zero data, while the second employs a regression calibration framework to utilize the full conditional distribution of $X_i(t)$. They are designed to adjust for the biases associated with estimation. While both are developed under the same model assumptions and are designed for the same application context, they differ in the technical approach used for recovering $X_i(t)$.

2.2.1 Pointwise two-stage mixed effect model approach

Mixed effect models have been previously demonstrated as an approach for adjusting for measurement error (Luan et al., 2023; Huo et al., 2025; Xie et al., 2018). For two-staged-based methods, such as regression calibration (Spiegelman et al., 1997; Hardin et al., 2003; Wang et al., 1997), $\mathbb{E}\{X_i(t) | W_{ij}(t), j = 1, \dots, J_i\}$ are often used as a prediction for $X_i(t)$ under certain assumptions and conditions. Here, we propose a pointwise mixed effect model-based method to obtain the prediction of $X_i(t)$ from its noisy and zero-inflated proxy $W_{ij}(t)$ via the idea of conditional expectation. While our method focuses on correcting for measurement error in zero-inflated functional predictors, it is partially inspired by the modular inferential framework proposed by Cui et al. (2022), which fits pointwise mixed models followed by functional smoothing and joint inference. We will explain why this method works and demonstrate that it employs the conditional expectation of X given W as the substitution.

From our statistical model we deduce that, for a fixed time point t , the observed variable $W_{ij}(t)$ is distributed as a mixture of a Gaussian distribution and a degenerate distribution:

$$W_{ij}(t) \sim \begin{cases} \mathcal{N}\left\{\frac{X_i(t)}{p_i(t)}, \sigma_u^2(t)\right\} & \text{with probability } p_i(t), \\ 0 & \text{with probability } 1 - p_i(t). \end{cases}$$

Let $W_{ij}^*(t)$ denote the non-zero observations of $W_{ij}(t)$. Based on our model assumptions, we can decompose $p_i(t) W_{ij}^*(t)$ as

$$p_i(t) W_{ij}^*(t) = \mu_x(t) + \left\{X_i(t) - \mu_x(t)\right\} + p_i(t) U_{ij}(t), \quad (4)$$

where for any fixed t , $\mu_x(t)$ is a constant, and both $\{X_i(t) - \mu_x(t)\}$ and $p_i(t) U_{ij}(t)$ are Gaussian with zero mean and are independent. Consequently, equation (4) corresponds to the following mixed effect model:

$$W_{ij} = b_0 + b_i + \varepsilon_{ij}, \quad (5)$$

subject to the distributional assumptions

$$\begin{aligned} b_i &\sim \mathcal{N}(0, d^2), \quad \text{Cov}(b_i, b_k) = 0 \quad \text{for all } i \neq k, \\ \varepsilon_{ij} &\sim \mathcal{N}(0, \sigma_i^2), \quad \text{Cov}(\varepsilon_{ij}, \varepsilon_{lm}) = 0 \quad \text{for } (i, j) \neq (l, m), \\ \text{Cov}(b_i, \varepsilon_{lm}) &= 0 \quad \text{for all } i, l, m. \end{aligned}$$

Here $\mathcal{W}_{ij} = p_i(t) W_{ij}^*(t)$ is the response; the fixed intercept b_0 represents $\mu_x(t)$; the individual-specific random effect b_i represents $X_i(t) - \mu_x(t)$; and the error term ε_{ij} represents $p_i(t) U_{ij}(t)$.

Assuming the $p_i(t)$ is known, we fit the Model (5) separately for each t . Let \hat{b}_0 denote the estimated b_0 and \hat{b}_i denote the prediction of b_i . The resulting predictor of $X_i(t)$ is then

$$\hat{X}_i(t) = \hat{b}_0 + \hat{b}_i.$$

For $p_i(t)$, we can use its estimate to replace it. And we will propose the method to estimate $p_i(t)$.

For mixed effect models, the best prediction of the random effect in terms of mean squared error is given by the conditional expectation of the random effect given the observed data (Chow, 2018). Therefore, this prediction represents the conditional expectation of $X(t)$ given the non-zero values of $W(t)$.

Note that the Model (5) does not satisfy the Gauss-Markov conditions due to heteroskedasticity, thus the variance of the error term ε_{ij} is not constant across observations and each individual may have a different variance. However, robust inference for fixed effects is well-established, and this heteroskedasticity does not compromise the quality of the estimates (Chow, 2018). Furthermore, simulation studies have demonstrated that the estimation of fixed effects and the prediction of random effects in mixed effect models are robust to violations of the underlying distributional assumptions (McCulloch and Neuhaus, 2011; Schielzeth et al., 2020). Consequently, by fitting the Model (5) using estimation methods developed under the Gauss-Markov conditions, we can generate reliable predictions for $X_i(t)$.

Estimation of $p_i(t)$. The \mathcal{W}_{ij} in Model (5) is defined as $p_i(t)W_{ij}^*(t)$ in equation (4). Recall that $p_i(t)$ denotes the activation probability at time t for subject i , representing the probability that the true latent process $X_i(t)$ is nonzero. Since $p_i(t)$ is latent, we replace $p_i(t)$ with its estimate $\hat{p}_i(t)$. Based on Model (2) and Model (3), we have $\text{logit}[\Pr\{W_{ij}(t) \neq 0\}] = (1, Z_i^\top)\theta(t)$. Therefore, we obtain $\hat{p}_i(t)$ by fitting the logistic regression model

$$\text{logit}\left(\Pr[I\{W_{ij}(t) \neq 0\}]\right) = (1, Z_i^\top)\theta(t), \quad (6)$$

for each t separately.

In the assumption (A1), we assume that $G_{ij}(t)$ can be correlated across j . If we assume $G_{ij}(t)$ are independent across j instead, we can use maximum likelihood methods to fit the model. Otherwise, we fit the logistic regression model by solving the generalized estimating equations (GEE). Alternatively, we can use $\hat{p}_i(t) = \frac{\sum_j I\{W_{ij}(t) \neq 0\}}{J_i}$ as the estimate of $p_i(t)$. This approach is mathematically equivalent to excluding the predictor Z_i and keeping only the intercept in the linear model described by equation (6). The advantage of the proportional approach is that it is simpler, distribution-free and remains valid even without assumption (A4), but the trade off is that it may be less efficient if covariates in Z_i truly predict the activation probability.

2.2.2 Pointwise regression calibration approach

The second approach adopts a regression calibration (Fuller, 2009) framework, which is a commonly used method to adjust for measurement error in predictors when fitting regression models. The key idea is to replace the unobserved true predictor with its conditional expectation given the observed, error-prone measurement. Specifically, if W denotes the observed predictor contaminated by error and X represents the true predictor, regression calibration approximates X by $\mathbb{E}(X | W)$ and uses this estimate in the regression analysis. This approach effectively reduces the bias introduced by measurement error, particularly in linear models. In nonlinear models, such as logistic regression,

regression calibration serves as an approximate correction and may still result in minor biases if the magnitude of measurement error is substantial (Carroll et al., 2006).

We propose a regression calibration estimation method that directly employs the conditional expectation of $X_i(t)$ given $W_{ij}(t)$ as the substitution for $X_i(t)$. In our previously proposed mixed-effects model-based approach, we estimate $p_i(t)$ based on whether $W_{ij}(t) = 0$, and use only the non-zero observations of $W_{ij}(t)$ to fit Model (5) for predicting $\hat{X}_i(t)$. Thus, the information from zero and non-zero values of $W_{ij}(t)$ is leveraged separately. In contrast, the regression calibration approach utilizes both zero and non-zero observations of $W_{ij}(t)$ jointly by modeling the full conditional distribution of $X_i(t)$ given $W_{ij}(t)$, offering a more unified and efficient strategy for measurement error correction. Wang et al. (2024) proposed a regression calibration method to address the issue of error-prone zero-inflated predictor in generalized linear model. This work extend their approach to functional data context and adapts it to accommodate the proposed relationship between the latent and observed variables. According to our assumptions, for each t , the marginal distribution of $X_i(t)$ is $X_i(t) \sim \mathcal{N}\{\mu_x(t), \sigma_x^2(t)\}$, and we have

$$\mathbb{E}\{X_i(t) \mid \widetilde{W}_i(t)\} = \frac{\int_{\mathcal{X}} x \prod_j \left(\left[p_i(t) \varphi\{W_{ij}(t) \mid x/p_i(t), \sigma_u^2(t)\} \right]^{\eta_{ij}(t)} \{1 - p_i(t)\}^{1-\eta_{ij}(t)} \right) \varphi\{x; \mu_x(t), \sigma_x^2(t)\} dx}{\int_{\mathcal{X}} \prod_j \left(\left[p_i(t) \varphi\{W_{ij}(t) \mid x/p_i(t), \sigma_u^2(t)\} \right]^{\eta_{ij}(t)} \{1 - p_i(t)\}^{1-\eta_{ij}(t)} \right) \varphi\{x; \mu_x(t), \sigma_x^2(t)\} dx}, \quad (7)$$

where $\widetilde{W}_i(t) = [W_{i1}(t), \dots, W_{iJ_i}(t)]^\top$, $\eta_{ij}(t) = I\{W_{ij}(t) \neq 0\}$, and $\varphi(x; \mu, \sigma^2)$ denotes the probability density function of $\mathcal{N}(\mu, \sigma^2)$. When we compute $\mathbb{E}\{X_i(t) \mid \widetilde{W}_i(t)\}$ using equation (7), we replace the unknown parameters with their estimates. For $p_i(t)$, we use the estimating method discussed in pointwise two-stage mixed effect model approach part (Section 2.2.1). For $\mu_x(t)$, $\sigma_x^2(t)$, and $\sigma_u^2(t)$, we propose the following estimators:

$$\begin{aligned} \hat{\mu}_x(t) &= \frac{\sum_i \sum_j W_{ij}(t)}{\sum_i J_i}, \quad \hat{\sigma}_x^2(t) = \frac{\sum_i \left[\hat{p}_i(t) \cdot \left\{ \bar{W}_{i\cdot}^*(t) - \bar{W}^*(t) \right\} \right]^2}{n^*(t) - 1}, \\ \hat{\sigma}_u^2(t) &= \frac{\sum_{i: r_i(t) > 1} \left(\left[\sum_j I\{W_{ij}(t) \neq 0\} \cdot \left\{ W_{ij}(t) - \bar{W}_{i\cdot}^*(t) \right\}^2 \right] / \{r_i(t) - 1\} \right)}{n_1^*(t)}, \end{aligned}$$

where

$$\begin{aligned} r_i(t) &= \sum_j I\{W_{ij}(t) \neq 0\}, \quad n^*(t) = \sum_i I\{r_i(t) \neq 0\}, \quad n_1^*(t) = \sum_i I\{r_i(t) > 1\}, \\ \bar{W}_{i\cdot}^*(t) &= \frac{\sum_j W_{ij}(t) I\{W_{ij}(t) \neq 0\}}{r_i(t)}, \quad \bar{W}^*(t) = \frac{\sum_{i: r_i(t) \neq 0} \bar{W}_{i\cdot}^*(t)}{n^*(t)}. \end{aligned}$$

While the integrals in the numerator and denominator appear complex, they are univariate and can be efficiently computed using Monte Carlo methods.

2.3 Scalar-on-function regression

Following the prediction step of $X(t)$ described in section 2.2, we address the computational challenges of functional regression by approximating $X(t)$ using a finite number of basis functions, thereby reducing the infinite-dimensional problem to a finite-dimensional one. For a generalized linear regression model that incorporates a functional predictor along with m scalar predictors, the

link between the expected value of the response variable and the predictors for an individual i is expressed by

$$g[\mathbb{E}\{Y_i|X_i(t), Z_i\}] = \int_{\Omega} \beta(t)X_i(t)dt + (1, Z_i^\top)\gamma,$$

where Ω denotes the temporal domain. For a complete basis of $L^2(\Omega)$ function space, denoted as $\{\rho_k\}_{k=1}^\infty$, there exists a sequence of coefficients $\{c_k\}_{k=1}^\infty$ such that $\int_{\Omega} \beta(t)X_i(t)dt = \int_{\Omega} \{\sum_{k=1}^\infty c_k \rho_k(t)\} X_i(t)dt = \sum_{k=1}^\infty c_k \int_{\Omega} \rho_k(t)X_i(t)dt$. We can perform truncation by selecting a finite subset of the basis and then use $\sum_{k=1}^K c_k \int_{\Omega} \rho_k(t)X_i(t)dt$ to approximate $\int_{\Omega} \beta(t)X_i(t)dt$. Then the scalar-on-function regression model above turns into

$$g[\mathbb{E}\{Y_i|X_i(t), Z_i\}] = \sum_{k=1}^K c_k \int_{\Omega} \rho_k(t)X_i(t)dt + (1, Z_i^\top)\gamma.$$

The term $\int_{\Omega} \rho_k(t)X_i(t)dt$ is then regarded as the predictors for the regression ($k = 1, \dots, K$), effectively transforming the problem into a scalar-on-scalar generalized linear regression problem. In practice, we don't necessarily need the basis functions to be orthogonal. We can employ other types of basis functions such as B-splines, provided they are not linearly dependent. We use $\frac{\|\Omega\|}{|\mathcal{T}|} \sum_{t \in \mathcal{T}} \rho_k(t)X_i(t)$ to numerically compute the value of the integral $\int_{\Omega} \rho_k(t)X_i(t)dt$ where $\|\cdot\|$ denote the Lebesgue measure, \mathcal{T} is the finite set of time points where $X_i(t)$ is measured, and $|\mathcal{T}|$ represents the cardinality of \mathcal{T} .

To provide theoretical support for the proposed regression framework, we analyze the asymptotic behavior of the proposed bias correction estimator in a scalar-on-function linear regression setting. Our main finding is stated in Theorem 2. Prior to proving Theorem 2 we first need to establish a preliminary result regarding the consistency of the least-squares estimator for the scalar-on-function linear regression model.

Consider the scalar-on-function linear regression model

$$Y_i = \int_{\Omega} X_i(t)\beta(t)dt + \varepsilon_i, \quad i = 1, \dots, n, \quad (8)$$

where Ω is a compact interval in \mathbb{R} , $\|\beta\|_{L^2(\Omega)} < \infty$, and ε_i are independent errors with $\mathbb{E}[\varepsilon_i] = 0$ and $\text{Var}(\varepsilon_i) = \sigma^2 < \infty$.

Let $\{\rho_k\}_{k=1}^\infty$ be a complete orthonormal basis of $L^2(\Omega)$. For each subject i and index k define $x_{ik} := \langle X_i, \rho_k \rangle = \int_{\Omega} X_i(t)\rho_k(t)dt$. Define $b_k := \langle \beta, \rho_k \rangle$ and $\boldsymbol{\theta}_K := (b_1, \dots, b_K)^\top$. Let $\tilde{\boldsymbol{\theta}}_K := (\tilde{b}_1, \dots, \tilde{b}_K)^\top$ denote the ordinary least square estimator of $\boldsymbol{\theta}_K$, obtained by regressing Y_i on x_{i1}, \dots, x_{iK} with the corresponding function estimate defined as $\tilde{\beta}_K(t) := \sum_{k=1}^K \tilde{b}_k \rho_k(t)$.

Lemma 1. *Let $\{(X_i, Y_i)\}_{i=1}^n$ be an i.i.d. sample generated from model (8). Estimate the regression function using the first $K = K_n$ basis functions of $\{\rho_k\}_{k=1}^\infty$, where the truncation level K_n is allowed to depend on n . Assume that*

- (B1) $K_n \rightarrow \infty$ and $K_n/n \rightarrow 0$ as $n \rightarrow \infty$;
- (B2) for every finite K , the covariance matrix $\Sigma_K := \text{Cov}(x_{i1}, \dots, x_{iK})$ is positive definite;
- (B3) $\mathbb{E}[\|X_i\|_{L^2(\Omega)}^2] < \infty$.

Then the least-squares estimator $\tilde{\beta}_{K_n}$ is L^2 -consistent for β on Ω , that is,

$$\|\tilde{\beta}_{K_n} - \beta\|_{L^2(\Omega)} \xrightarrow{P} 0, \quad n \rightarrow \infty.$$

(Undefined notation is summarized in Section [Appendix A](#).)

Lemma 1 is a well-known classical result establishing the consistency of the least-squares estimator for the scalar-on-function linear regression model. Its proof is therefore omitted.

We introduce an auxiliary process $W_{ij}(t)$, observed on a finite grid $\mathcal{T}_m \subset \Omega$, which acts as a functional proxy for the latent predictor $X_i(t)$ in model (8). The proxy mechanism is governed by the following assumptions:

- (C1) For every fixed $t \in \Omega$, the conditional variables $\{W_{ij}(t) \mid X_i(t) = x\} \sim F_{W|X,t}(\cdot \mid x, t)$ are i.i.d. over $j = 1, \dots, J_i$.
- (C2) The collections $\{X_i, Y_i, \{W_{ij}\}_j\}_{i=1}^n$ are i.i.d. over $i = 1, \dots, n$.
- (C3) (Identifiability) For any fixed $t \in \Omega$ and $x_1 \neq x_2$, $F_{W|X=x_1,t} \neq F_{W|X=x_2,t}$.
- (C4) Conditional independence: $Y_i \perp\!\!\!\perp W_i \mid X_i$.

Let $\{\mathcal{T}_m\}_{m \geq 1}$ be a sequence of finite grids $\mathcal{T}_m = \{t_{m,1}, \dots, t_{m,m}\} \subset \Omega$. Let $t_{(0)} < t_{(1)} < \dots < t_{(m+1)}$ denote the increasing arrangement of the grid points in \mathcal{T}_m together with the endpoints of Ω . Define the mesh width as $\Delta_m := \max_{1 \leq j \leq m+1} \{t_{(j)} - t_{(j-1)}\}$. For every i and $t \in \mathcal{T}_m$ write $W_i(t) := [W_{i1}(t), \dots, W_{iJ_i}(t)]^\top$. Define $\widehat{X}_i(t) := \mathbb{E}\{X_i(t) \mid W_i(t)\}$. For each i and k , define estimated basis scores as $\hat{x}_{ik} := \frac{\|\Omega\|}{|\mathcal{T}_m|} \sum_{t \in \mathcal{T}_m} \widehat{X}_i(t) \rho_k(t)$. Let $\widehat{\boldsymbol{\theta}}_K := (\widehat{b}_1, \dots, \widehat{b}_K)^\top$ denote the least-squares estimator of $\boldsymbol{\theta}_K$, obtained by regressing Y_i on $\hat{x}_{i1}, \dots, \hat{x}_{iK}$ with the corresponding function estimate defined as $\widehat{\beta}_K(t) := \sum_{k=1}^K \widehat{b}_k \rho_k(t)$. We call $\widehat{\beta}_K(t)$ a plug-in estimator because it is obtain from plugging $\widehat{X}_i(t)$ as the substitution of $X_i(t)$ into the least-squares estimator $\widetilde{\beta}_K(t)$.

Theorem 2. Consider model (8) under assumptions (C1)–(C4) together with the conditions of Lemma 1. Let

$$\{Y_i, W_{ij}(t) : t \in \mathcal{T}_m, j = 1, \dots, J_i\}_{i=1}^n$$

be the observed sample, and estimate β using the first K_n basis functions. If, in addition,

- (D1) $\Delta_m \rightarrow 0$ ($m \rightarrow \infty$);
- (D2) $\inf_i J_i \rightarrow \infty$;
- (D3) for every n and K , both design matrices

$$\widehat{\mathbf{X}}_K := (\hat{x}_{ik})_{n \times K}, \quad \mathbf{X}_K := (x_{ik})_{n \times K}$$

have full column rank.

Then the plug-in estimator $\widehat{\beta}_{K_n}$ is L^2 -consistent on Ω ; that is,

$$\|\widehat{\beta}_{K_n} - \beta\|_{L^2(\Omega)} \xrightarrow{P} 0 \quad \text{as } n \rightarrow \infty, \inf_i J_i \rightarrow \infty, m \rightarrow \infty.$$

(Undefined notation is summarized in Section [Appendix A](#).)

The proof of Theorem 2 is given in Section [Appendix B](#).

In the Section 2.2, we explained that both of our proposed estimators for $X_i(t)$ are built on the surrogate predictor $\mathbb{E}[X \mid W]$. Theorem 2 further establishes that the resulting plug-in estimator is consistent for the scalar-on-function linear regression model. For the broader class of generalized linear models (GLMs), estimation is typically carried out via maximum likelihood, with the choice of response distribution and link function determining the specific procedure. In these settings the same consistency result continues to hold, and the proofs follow similar arguments along those presented here. Due to limited space, the specifics of these proofs are not provided here.

3 Simulation study

To evaluate the finite sample performance of our proposed methods, we performed several simulation studies under various controlled settings. Specifically, we examined the accuracy of parameter estimation and the robustness of our methods under various levels of measurement error and different data-generating conditions, such as sample size, predictor correlation, and the prevalence

of zero values. We compared our proposed mixed model based- and regression calibration-based approaches with other methods, including the (i) Naive average method which uses $\bar{W}_i(t)$ as the substitution of $X_i(t)$; (ii) Non-zero-inflated mixed model based method. This is also a mixed-effects model-based method. However, unlike the proposed approach in this article, it applies mixed-effects modeling without accounting for zero inflation. To distinguish it from the mixed model-based method proposed in Section 2.2, we refer to this comparison approach as the "non-zero-inflated mixed model-based" / "non-ZI mixed model-based" / "non-ZI MM" method, while the mixed model-based method in Section 2.2 is referred to as the "zero-inflated mixed model-based" / "ZI mixed model-based" / "ZI MM" method, or simply the "mixed model-based" / "MM" method. [Luan et al. \(2023\)](#) previously explored this method. Our methods were also compared to the naive one day method which uses the first replicate of each individual, $W_{i1}(t)$, as the substitution of $X_i(t)$. We note that while we used the first replicate, the replicate for another day may also be employed for this approach. Additionally, we compared our methods with the benchmark approach which uses the true value of $X(t)$, highlighting the effectiveness of our scalar-on-function regression algorithm.

We fit two distinct methods within the framework of our proposed mixed effects model and regression calibration approaches:

- (i) **Pointwise approach:** Apply the model specified in equation (6) to each t in order to determine $\theta(t)$, and subsequently use the estimated value $\hat{\theta}(t)$ in conjunction with Z_i to compute $p_i(t)$.
- (ii) **Smoothed pointwise approach:** Similar to the pointwise method, fit the model in equation (6) for each t to find $\theta(t)$, but smooth $\hat{\theta}(t)$ over t before combining it with Z_i to derive $p_i(t)$. The pointwise approach offers flexibility and can capture local variations in $\theta(t)$, but it may yield noisy and unstable estimates. In contrast, the smoothed pointwise approach reduces variance and improves interpretability by borrowing strength across nearby time points, though it may introduce bias if $\theta(t)$ has abrupt changes. The choice depends on the expected smoothness of $\theta(t)$ and the trade-off between bias and variance.

3.1 Simulation Settings

We now detail the data-generating mechanisms used in our simulation study. For evaluating the varying effects of the sample size n , we used $n = 50, 100, 200, 500, 1000$. The number of measurement replicates for each subject, J_i , is uniformly set to 7. for all i . The time domain Ω is set as $[0, 1]$, within which we collect functional predictor measurements at 24 evenly spaced time points. Although in practice accelerometer based functional data are mostly minute-level, we used 24 equally spaced time points to represent a daily trajectory in our simulation study. This coarse grid was chosen for computational efficiency and clarity of illustration. Since the proposed method operates pointwise over time, its performance is not sensitive to the temporal resolution, provided that the underlying functional pattern is adequately captured.

We generate two error-free scalar predictors, denoted as Z_c and Z_b . The predictor Z_c follows a normal distribution $\mathcal{N}_n(0, \sigma_c^2 I_n)$, while Z_b follows a binomial distribution $\text{Binom}(n, p_b)$. We let $\sigma_c^2 = 1$ and $p_b = 0.6$. For γ in Model (1), the chosen parameters are $(5, 0.2, 0.4)^\top$, where the first value represents the intercept, and the second and third values denote the slopes for the scalar predictor Z_c and Z_b .

Given the two scalar predictors Z_c and Z_b , the vector $\theta(t)$ is composed of three components: $\theta(t) = [\theta_0(t), \theta_c(t), \theta_b(t)]^\top$. Each component, namely $\theta_0(t)$, $\theta_c(t)$, and $\theta_b(t)$, is derived using a stationary Gaussian process $\vartheta(t)$ with a mean of 0 and a variance of 1. The correlation is modeled by the function $\kappa(s, t) = \exp\{-\frac{(s-t)^2}{0.45}\}$. The value assigned to each $\theta(t)$ component is in the form $a + d \cdot \Phi(\vartheta(t))$, where Φ^{-1} represents the inverse cumulative distribution function of a standard normal distribution. The generation of each component of $\theta(t)$ follows this independent yet identical approach, leading to an interval for $\theta(t)$'s components of $(a, a + d)$ across all $t \in \Omega$. For the simulation, we vary the zero value proportion in W through adjustments in a and d . Specifically, d

is set to 0.2, 0.8, and 1 for $\theta_0(t)$, $\theta_c(t)$, and $\theta_b(t)$, respectively. The offset a is set to -0.4 and -0.5 for $\theta_c(t)$ and $\theta_b(t)$, respectively, with multiple settings of 0.3, 0.6, 0.8, 1 for $\theta_0(t)$. Once the Z and $\theta(t)$ are generated, the $p_i(t)$ can be calculated. The resulting anticipated zero-value proportions in W are 0.403, 0.335, 0.294, and 0.255.

In the model, we assume that $X_i(t)$ are i.i.d Gaussian process over i . We did not specify the form of the mean and covariance function for $X_i(t)$. In the simulation study, for each individual i , we simulate $X_i(t)$ as a Gaussian process with a mean given by $\mathbb{E}\{X_i(t)\} = 4 + \sin(1 + 2.8\pi t)$ and a covariance described by $\text{Cov}(X_s(t), X_i(s)) = \{1 + 0.1 \cos(-1 + 2.8\pi t)\} \cdot \exp\{-\frac{25(s-t)^2}{2}\}$. In this covariance function, the term $1 + 0.1 \cos(-1 + 2.8\pi t)$ defines a time-varying variance, while the Gaussian kernel $\exp\{-\frac{25(s-t)^2}{2}\}$ specifies a smooth correlation structure. This construction introduces mild nonstationarity while preserving local dependence, reflecting realistic features of functional data. The functional parameter $\beta(t)$ is defined as $\beta(t) = \sin(2\pi t)$. We generate $G_{ij}(t)$ according to the equation:

$$G_{ij}(t) = q_g G_{0,i}(t) + \sqrt{1 - q_g^2} G_{1,ij}(t), \quad (9)$$

where $\{G_{0,i}(t), t \in \Omega\}$ and $\{G_{1,ij}(t), t \in \Omega\}$ are independent, stationary Gaussian processes for every i and j , with properties: $\mathbb{E}\{G_{0,i}(t)\} = \mathbb{E}\{G_{1,ij}(t)\} = 0$ and $\text{Var}\{G_{0,i}(t)\} = \text{Var}\{G_{1,ij}(t)\} = 1$, for all $t \in \Omega$; where $0 \leq q_g < 1$. Both $G_{0,i}(t)$ and $G_{1,ij}(t)$ are modeled and simulated as stationary Gaussian processes with a mean of zero, a variance of one, and a correlation function given by $\kappa(s, t) = \exp\{-50(s-t)^2\}$. Various values for q_g such as 0, 0.2, and 0.4 were used. The term q_g controls the proportion of shared structure in the latent variable $G_{ij}(t)$, determining the correlation between different j for the same i , and thus shaping the dependency structure of $I\{W_{ij}(t) \neq 0\}$. A larger q_g leads to stronger correlations in whether $W_{ij}(t) = 0$ across j , while $q_g = 0$ implies that these events are independent.

The $U_{ij}(t)$ in the model is a zero-mean Gaussian process, thus, so it suffices to specify its covariance function for simulation. The covariance function can be expressed in the form $\sigma(s)\sigma(t)\kappa(s, t)$, where $\sigma(\cdot)$ denotes the pointwise standard deviation function and $\kappa(s, t)$ is a correlation function that captures the dependence structure between time points s and t . In our simulation, we implement a constant function, $\sigma(t) = \sigma_u$, for $U_{ij}(t)$ and used several constant values for σ_u , including 1, 2, and 3. Several types of correlation function κ are considered:

- (i) **Squared exponential:** $\kappa(s, t) = \exp\left\{-\frac{(t-s)^2}{2\rho_u^2}\right\},$
- (ii) **Spatial power:** $\kappa(s, t) = \rho_u^{|t-s|}, \quad 0 < \rho_u < 1,$
- (iii) **Two-value:** $\kappa(s, t) = \begin{cases} 1 & \text{if } s = t \\ \rho_u & \text{else} \end{cases}, \quad 0 < \rho_u < 1.$

The corresponding covariance structures are autoregressive of order 1 (AR(1)) for the spatial power function and compound symmetry (also known as exchangeable correlation) for the two-value function. For each correlation function, we used different values for the parameter ρ , which controls the strength and decay rate of the correlation over time t (or location s and t): for the squared exponential correlation, $\rho = 0.1, 0.15, 0.2$; for the spatial power correlation, $\rho = 0.2, 0.4, 0.6$; and for the two-value correlation, $\rho = 0.2, 0.4, 0.6$.

We calculate the $W_{ij}(t)$ once the $X_i(t)$, $U_{ij}(t)$, $G_{ij}(t)$, and $p_i(t)$ are generated. After selecting the link function $g(\cdot)$, the type of distribution EF, and the dispersion parameter ϕ , the response variable can also be simulated. The specified link function $g(\cdot)$ allows for the computation of μ_i , which is the conditional expectation of Y_i given $X_i(t)$ and Z_i . We simulate Y_i with the specified values of ϕ and EF.

In the simulation study, we generate two different types of response variable Y :

(i) **Continuous**: The distribution EF is (unidimensional) Gaussian distribution. For this case, the link function $g(\cdot)$ used is identity function. Then we have

$$Y_i = \int_{\Omega} \beta(t) X_i(t) dt + (1, Z_i^\top) \gamma + \varepsilon_i$$

where $(\varepsilon_1, \dots, \varepsilon_n)^\top \sim \mathcal{N}_n(0, \sigma_0^2 I_n)$. The ϕ is corresponding to the σ_0^2 . In this case, we use 0.02 as the value of σ_0^2 .

(ii) **Binary**: The distribution EF is Bernoulli distribution. For this case, the link function $g(\cdot)$ used is logit function. Then we have

$$\Pr(Y_i = 1) = \int_{\Omega} \beta(t) X_i(t) dt + (1, Z_i^\top) \gamma.$$

There is no ϕ that we need to specify its value.

In our simulation studies, several factors were varied including: the sample size (default: 100); the proportion of zero values in W (default: 0.335); the scale of the deviation of the measurement error term U , denoted by σ_u (default: 1); and the correlation structure of U , including both the type of correlation function and the parameter ρ_u within it (default: squared exponential correlation function with $\rho_u = 0.2$). We also varied the types of response variable and the value of q_g in equation (9) (default: 0). We investigated the effects of these factors on estimation result. Although the probability of zero values in $W(t)$ cannot be directly specified by a single parameter, it is implicitly controlled through the choice of the function $\theta(t)$ in Model (3).

In our simulation studies, we focus on the estimation of the functional parameter $\beta(t)$, as it is directly associated with the error-prone functional predictor $X(t)$ and is of primary inferential interest in our modeling framework. The bias and variance of the estimate of functional parameter β are defined as follows:

$$\text{Bias: } \left[\int_{\Omega} \left\{ \mathbb{E} \widehat{\beta}(t) - \beta(t) \right\}^2 dt \right]^{\frac{1}{2}} \quad (10)$$

$$\text{Variance: } \int_{\Omega} E \left[\widehat{\beta}(t) - \mathbb{E} \{ \widehat{\beta}(t) \} \right]^2 dt \quad (11)$$

where $\widehat{\beta}(t)$ is the estimate of $\beta(t)$. We use the defined bias and variance to evaluate the goodness of the estimate for β .

3.2 Simulation Results

Figure 1 shows the average $\widehat{\beta}(t)$ of different estimation methods versus the true $\beta(t)$ under the default simulation setting: sample size $n = 100$, zero proportion in $W(t) \approx 0.335$, measurement error scale $\sigma_u = 1$, $q_g = 0$, and squared exponential correlation function for $U(t)$ with $\rho_u = 0.2$.

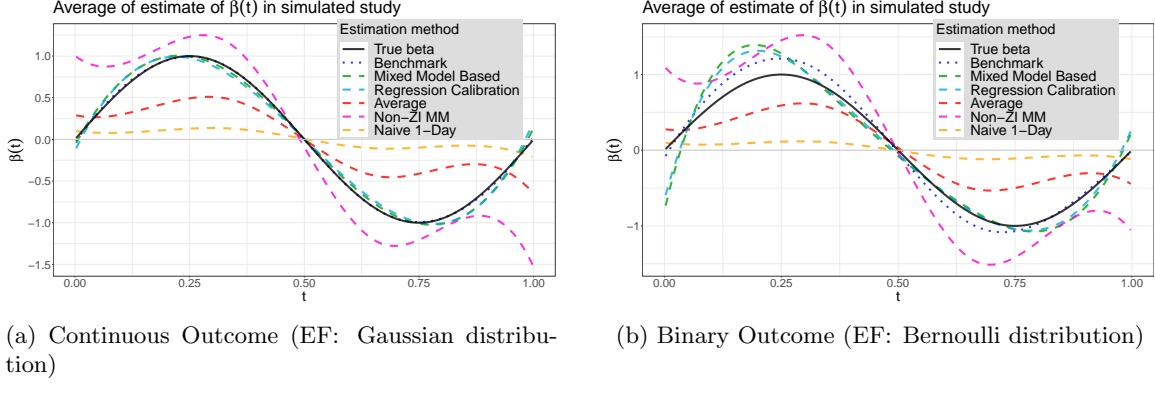


Figure 1: True $\beta(t)$ (black solid) and the average estimated $\hat{\beta}(t)$ (colored lines) under different methods in simulation study. (Non-ZI MM = non-zero-inflated mixed model based method.) **Common simulation settings (continuous outcome):** conditional distribution of $Y|X(t), Z$: Gaussian distribution (with identity link); sample size: $n = 100$; estimation method of $\theta(t)$: pointwise; proportion of zero values: $\mathbb{E}\{\Pr(W_{ij}(t) = 0)\} \approx 0.335$; Covariance function of $U(t)$: squared-exponential with $\rho_u = 0.2$, $\sigma_u = 1$; $q_g = 0$. **Common simulation settings (binary outcome):** conditional distribution of $Y|X(t), Z$: Bernoulli distribution (with logit link); other settings identical.

With all other settings held constant based on the values used for Fig .1, while changing the sample size N , we obtained the results in the Table 1. Table 1 (a) and Table 1 (c) demonstrates the average squared bias of $\hat{\beta}(t)$ for different estimation methods defined in equation (10). Table 1 (b) and Table 1 (d) shows the average variance of $\hat{\beta}(t)$ for different estimation methods defined in equation (11). The Fig .1 and Table 1 present a subset of our simulation study results under a common model setting but with varying sample sizes. Additional results under various settings are provided in the Section [Appendix C](#), further demonstrating the robustness of the proposed methods across a wide range of scenarios. These scenarios encompass logistic regression models for the outcome, varying scales and error structures in the measured predictor, the use or omission of smoothing in estimating $\theta(t)$, and differing proportions of zero values in W .

Our simulation results indicate that the naive average approach significantly attenuates the estimation of $\beta(t)$. The "naive 1 day" method results in even more substantial attenuation. Additionally, the "no zero inflation" method yields a biased estimate for β . To address this, our bias correction techniques, including the mixed model-based and the regression calibration methods, can mitigate the extent of bias in the estimation of $\beta(t)$. However, the "non-ZI MM" method, which is the mixed-model-based bias correction approach without accounting for zero inflation, produces highly unstable estimates (with high variance) when the sample size is small. The trade-off associated with our proposed bias correction methods is an increase in estimation variance, which corresponds to reduced efficiency. When comparing our two proposed bias correction methods, the mixed model approach yields less bias than the regression calibration approach when sample sizes are large, but more bias when sample sizes are small. Conversely, the regression calibration method results in lower variances for the estimated coefficient functions. Furthermore, in terms of computational speed, the mixed model method outperforms the regression calibration approach.

Table 1: Simulation results for six estimation methods across different sample sizes N . Top two panels: continuous outcome; bottom two panels: binary outcome. Each pair shows average squared bias (first) and average variance (second). **Common simulation settings (continuous outcome):** conditional distribution of $Y|X(t), Z$: Gaussian distribution (with identity link); estimation method of $\theta(t)$: pointwise; proportion of zero values: $\mathbb{E}\{\Pr(W_{ij}(t) = 0)\} \approx 0.335$; Covariance function of $U(t)$: squared-exponential with $\rho_u = 0.2$, $\sigma_u = 1$; $q_g = 0$. **Common simulation settings (binary outcome):** conditional distribution of $Y|X(t), Z$: Bernoulli distribution (with logit link); other settings identical. **Benchmark** = benchmark method; **Average** = naive average method; **MM** = mixed model based method proposed in Section 2.2; **RC** = regression calibration method proposed in Section 2.2; **Non-ZI MM** = non-zero-inflated mixed model based method; **1 day** = naive one-day method.

(a) Continuous Y : Average Squared Bias						
N	Benchmark	MM	RC	Average	Non-ZI MM	1 day
50	0.0001213	0.003945	0.005530	0.1497	0.2995	0.3897
100	0.0000903	0.003446	0.005038	0.1445	0.1689	0.3822
200	0.0001204	0.003259	0.005246	0.1489	0.1318	0.3840
500	0.0001262	0.002772	0.004994	0.1468	0.1190	0.3842
1000	0.0001110	0.002619	0.004417	0.1494	0.1225	0.3846

(b) Continuous Y : Average Variance						
N	Benchmark	MM	RC	Average	Non-ZI MM	1 day
50	0.0023843	0.135181	0.120203	0.0586	2.6930	0.0190
100	0.0010200	0.061922	0.049800	0.0269	0.3297	0.0085
200	0.0005190	0.034514	0.026972	0.0155	0.1311	0.0047
500	0.0002088	0.014465	0.010488	0.0069	0.0479	0.0018
1000	0.0000995	0.008700	0.005136	0.0046	0.0246	0.0010

(c) Binary Y : Average Squared Bias						
N	Benchmark	MM	RC	Average	Non-ZI MM	1 day
50	0.0001213	0.003914	0.005610	0.1497	0.2995	0.3897
100	0.0000903	0.003400	0.005045	0.1445	0.1689	0.3822
200	0.0001204	0.003118	0.005186	0.1489	0.1318	0.3840
500	0.0001262	0.002646	0.004883	0.1468	0.1190	0.3842
1000	0.0001110	0.002508	0.004310	0.1494	0.1225	0.3846

(d) Binary Y : Average Variance						
N	Benchmark	MM	RC	Average	Non-ZI MM	1 day
50	0.0023843	0.135726	0.119692	0.0586	2.6930	0.0190
100	0.0010200	0.062859	0.050002	0.0269	0.3297	0.0085
200	0.0005190	0.034582	0.026807	0.0155	0.1311	0.0047
500	0.0002088	0.014532	0.010509	0.0069	0.0479	0.0018
1000	0.0000995	0.008773	0.005209	0.0046	0.0246	0.0010

4 Application to School-Based Intervention Data from Texas, US

Having demonstrated the performance of the proposed method through simulation studies, we now apply it to a real dataset to illustrate its practical utility. Our objectives are (i) to evaluate how the method performs under realistic conditions, (ii) to examine the consistency between our proposed bias correction approaches, (iii) to determine whether they yield results that differ significantly from those produced by alternative methods. The dataset used in this application was collected from a

school-based intervention study conducted in Texas, United States, which investigated the impact of stand-biased desks on children’s health outcomes. Here, we use this dataset to illustrate the application of our statistical method.

Childhood obesity remains a pressing public health issue in the United States. Between 1999–2000 and 2021–2023, its prevalence among children and adolescents aged 2–19 years rose from 13.9% to 21.1%, while severe obesity doubled from 3.6% to 7.0% ([Centers for Disease Control and Prevention \(CDC\), 2020](#)). This trend is concerning due to its association with persistent obesity into adulthood ([Simmonds et al., 2016](#)) and reduced life expectancy ([Dietz, 1998; Mossberg, 1989](#)). Traditional classroom environments, where students remain seated for long periods, contribute to sedentary behavior and may exacerbate the problem. To address this, researchers at Texas A&M University, led by Dr. Mark Benden, launched a series of studies beginning in 2009 to evaluate the impact of stand-biased desks in elementary schools ([Benden et al., 2011](#)). These studies examined whether modifying classroom environments could promote physical activity, increase energy expenditure, and reduce the body mass index (BMI) among students. Results showed that students using stand-biased desks had significantly higher energy expenditure and step counts during class compared to those in traditional seated classrooms ([Benden et al., 2011, 2014](#)). A follow-up study further reported a significant reduction in BMI percentiles among students who used stand-biased desks for two consecutive years relative to those who remained in seated classrooms ([Wendel et al., 2016](#)). These findings suggest that redesigning classroom settings to incorporate stand-biased desks may serve as an effective, school-based intervention for reducing sedentary time and addressing childhood obesity.

Leveraging data from the Texas elementary school intervention studies, we apply our proposed analytical method to evaluate its effectiveness in extracting meaningful insights from real-world settings. The dataset includes key health and behavioral metrics, such as changes in BMI, energy expenditure, and physical activity levels measured via wearable accelerometers. A notable characteristic of the step count data is its zero-inflation: a substantial proportion of observations are zeros, with the proportion varying markedly across both time points and individuals. This pattern aligns with a key assumption of our model, that the probability of observing a zero depends on both time and individual-specific factors—as illustrated in Figure 2.

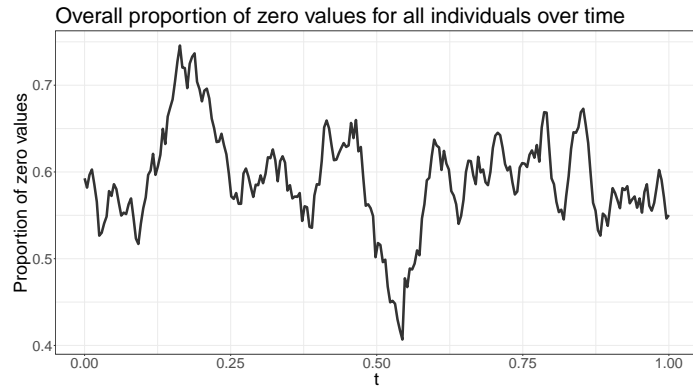


Figure 2: The proportion of zero values of individuals in the step count data collected from elementary school children by Benden et al.

We focus on two primary outcomes: the change in BMI over the study period (*delta_BMI*, a continuous variable), and an indicator of whether a participant’s BMI decreased during the study (*BMI_reduced*, a binary outcome). For each participant, these outcomes were derived from anthropometric measurements taken at the beginning and end of their intervention period. This setting offers an ideal case study for evaluating the impact of classroom-based interventions, such as stand-biased desks, on child health. By applying our modeling framework, we aim to identify patterns

in the data, assess the intervention's effectiveness, and demonstrate the practical applicability of our approach for addressing public health questions in real-world educational environments. The following analysis showcases how our method processes, models, and interprets the data.

In this study, participants wore wearable devices for three to seven days. We focused on minute-level activity data recorded between 10:00 AM and 2:00 PM on each day the device was worn. For analysis, only data within this four-hour window were retained. To facilitate functional data analysis, we linearly rescaled the time variable such that 10:00 AM corresponds to 0 and 2:00 PM to 1, mapping all measurements to the unit interval [0, 1].

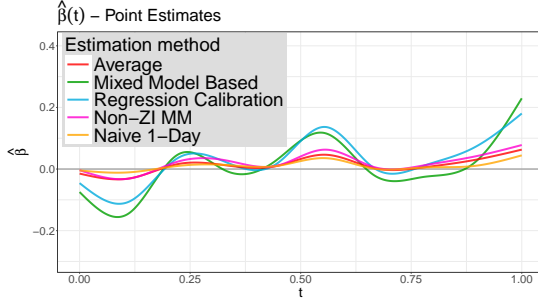
We applied the proposed bias correction methods, along with the comparison methods from the simulation study, to estimate the effect of step count on health outcomes among elementary school children, adjusting for age, sex, and ethnicity. These methods were previously evaluated through simulation to assess their relative performance. The full models are specified as follows:

$$\text{delta_BMI} = \int_{\Omega} \beta(t) \text{step count}(t) dt + \gamma_0 + \gamma_1 \text{age} + \gamma_2 \text{gender} + \gamma_{\text{ethnicity}} + \varepsilon,$$

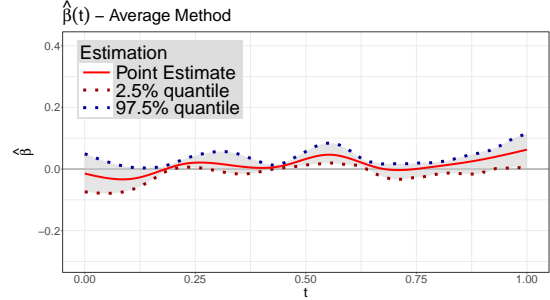
$$\text{logit Pr(BMI_reduced)} = \int_{\Omega} \beta(t) \text{step count}(t) dt + \gamma_0 + \gamma_1 \text{age} + \gamma_2 \text{gender} + \gamma_{\text{ethnicity}} + \varepsilon.$$

We used bootstrap sampling to construct pointwise confidence intervals for the estimated coefficient function $\beta(t)$.

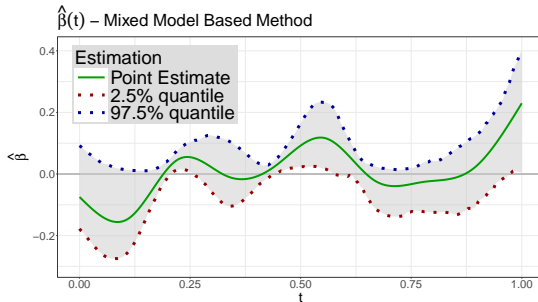
Figures 3 and 4 present the main application results. Figures 3 (a) and 4 (a) display the estimated coefficient functions $\beta(t)$, representing the effect of step count on *delta_BMI* and *BMI_reduced*, respectively. Figures 3 (b)-3 (f) and 4 (b)-4 (f) show the point estimates and confidence intervals of $\hat{\beta}(t)$ obtained from the various methods described in the simulation study for these two outcomes. The results in Figures 3 and 4 demonstrate strong agreement between our two proposed bias correction methods, while also revealing substantial differences compared to the other methods. In particular, the results highlight clear distinctions between methods that account for zero inflation and those that do not, underscoring the importance of explicitly modeling zero inflation in this context. Across all methods, the estimated coefficient functions $\hat{\beta}(t)$ for step count displayed certain time intervals where the pointwise bootstrap confidence intervals did not include zero, indicating statistically significant time-specific associations. The locations of these significant intervals were broadly similar across methods, while the proposed bias correction methods yielded effect estimates with smaller absolute magnitudes than the others—consistent with the expected attenuation from correcting for measurement error and zero inflation. For the scalar predictors (age, sex, and ethnicity), the estimated effects were small in magnitude and their confidence intervals included zero for all methods, indicating no statistically significant associations with either outcome. This lack of significance is likely due to the short follow-up period of no more than two weeks for each participant, during which substantial changes in BMI were unlikely to occur, as well as the relatively homogeneous distributions of these demographic variables in the sample, which limit variability for detecting associations. Nevertheless, it is important to include these predictors in the model, as they are established demographic and clinical covariates that may confound or modify the association of interest. Adjusting for them ensures that the estimated effect of step count is not biased by these background factors and can also improve statistical efficiency, even if their individual effects are not statistically significant in this dataset (Etminan et al., 2021; Morris et al., 2022). Although the time-varying proportion of zero values is plotted in Figure 2 for reference, its trend does not exhibit pointwise correspondence with the estimated $\beta(t)$. This is expected, as $\beta(t)$ is estimated as a single smooth function, where the value at each time point depends not only on local information but also on data across the entire time domain. Therefore, the differences in $\beta(t)$ reflect changes in the global modeling structure, rather than being solely driven by local zero proportions. Overall, these findings demonstrate the effectiveness of our proposed methods in real-world applications. We conclude with a summary of key results and a discussion of their broader implications.



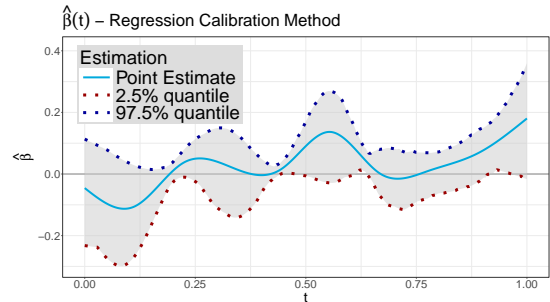
(a) Point estimate from Average, mixed model, and regression calibration method



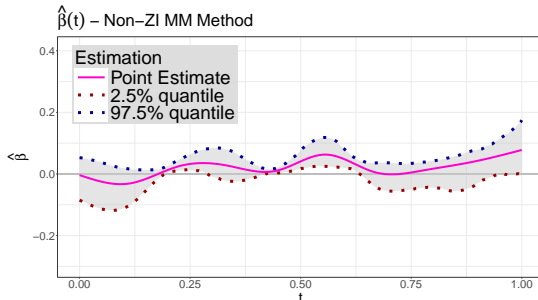
(b) Estimate and confidence interval from average method



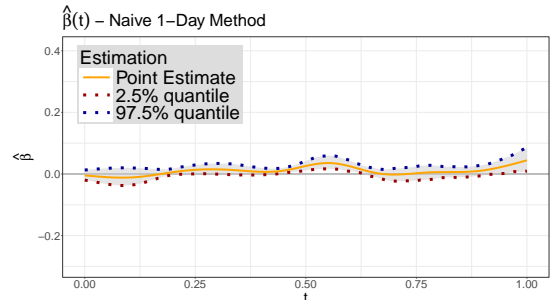
(c) Estimate and confidence interval from mixed model based method



(d) Estimate and confidence interval from regression calibration method

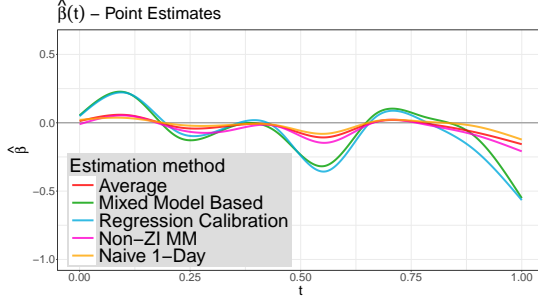


(e) Estimate and confidence interval from no zero inflation mixed model based method

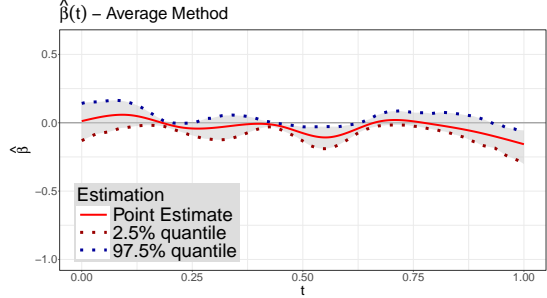


(f) Estimate and confidence interval from one-day method

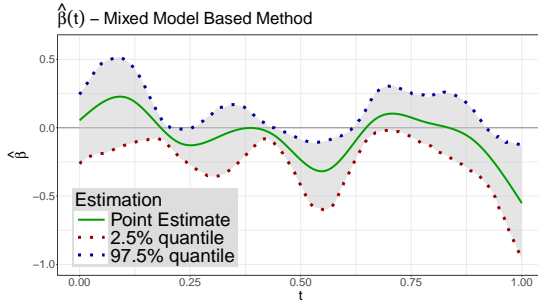
Figure 3: Estimated effect of step counts on $\delta\text{elta_BMI}$ adjusted for age, sex, and ethnicity. Panel (a) shows the point estimate from different methods. Panels (b)–(f) show the point estimate and confidence interval of $\hat{\beta}(t)$ from each method. Panels (c) and (d) correspond to our proposed bias correction methods.



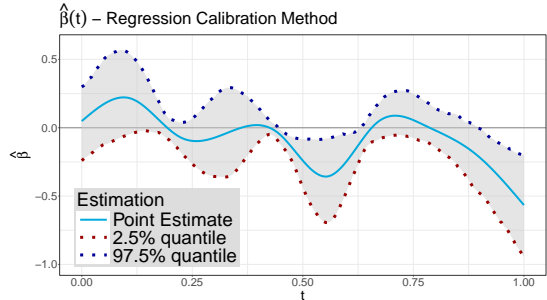
(a) Point estimate from Average, mixed model, and regression calibration method



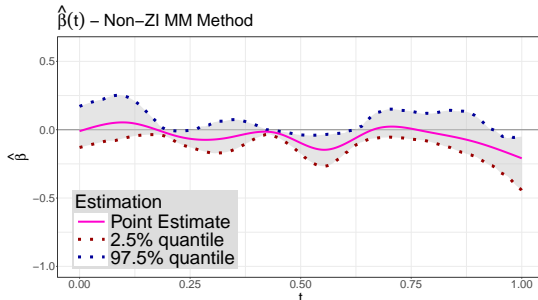
(b) Estimate and confidence interval from average method



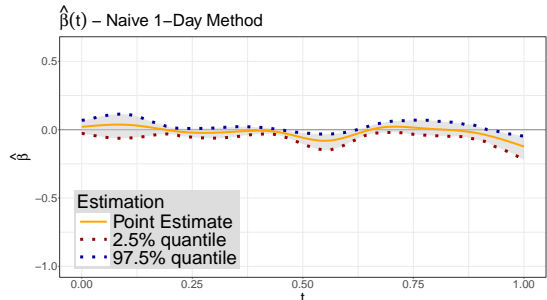
(c) Estimate and confidence interval from mixed model based method



(d) Estimate and confidence interval from regression calibration method



(e) Estimate and confidence interval from no zero inflation mixed model based method



(f) Estimate and confidence interval from one-day method

Figure 4: Estimated effect of step counts on *BMI-reduced* adjusted for age, sex, and ethnicity. Panel (a) shows the point estimate from different methods. Panels (b)–(f) show the point estimates and confidence intervals of $\hat{\beta}(t)$ from each method. Panels (c) and (d) correspond to our proposed bias correction methods.

5 Conclusion and Discussion

In this paper, we proposed a novel statistical framework for generalized linear regression with a scalar response and a zero-inflated error-prone functional predictor. The model is applicable to settings where a function-valued predictor is prone to both zero inflation and measurement errors such as step counts monitored by wearable devices. The model accommodates key challenges including excess zeros and measurement error in time-varying predictors through a semi-continuous modeling structure that leverages functional data techniques.

We developed two pointwise bias correction methods for parameter estimation: a mixed effects model-based approach and a regression calibration approach. Their performances were evaluated through extensive simulation studies and compared with several alternative estimation methods that do not address the measurement error or zero inflation issues. Results demonstrate that both proposed approaches substantially reduce estimation bias relative to the alternatives. Between the two, the mixed model-based method achieves lower bias and faster computation, while the regression calibration method exhibits better performance in terms of variance. The overall computational burden is acceptable in practice, and parallelization can be employed to further improve efficiency. These complementary strengths make the two approaches suitable for different practical scenarios, depending on the desired trade-off between bias, variance, and computational efficiency.

The scalar-on-function regression methods have been implemented in the R package `MECfda` (Ji et al., 2025), which also includes support for certain measurement error correction techniques (excluding the one proposed in this paper). The new methods introduced in this paper will be incorporated into future versions of the package.

The proposed estimation procedures are pointwise in nature, offering two main advantages. First, they reduce computational cost relative to methods that jointly model multiple time points. Second, they are more robust to violations of assumptions such as temporal correlation structures. However, a limitation of pointwise methods is their inability to exploit the full joint distribution of the functional predictor, which may affect statistical efficiency.

We applied our proposed methods to data collected from a cohort of children in Texas, drawn from a school-based childhood obesity intervention study that included health and behavioral measurements. Our analysis uncovered meaningful associations between physical activity (step count) and BMI outcomes, while accounting for measurement error and zero inflation—features commonly present in real-world accelerometer data.

Several avenues exist for extending our framework. In this study, we modeled the marginal distribution of the functional predictor at each time point as a mixture of a Gaussian and a point mass at zero. Future work could explore more flexible distributions beyond the Gaussian to better capture real-world variability. Additionally, developing estimation procedures that account for cross-time dependencies may improve statistical efficiency by leveraging the full joint distribution of the functional predictor. Bayesian approaches may enhance model flexibility, uncertainty quantification, and robustness in sparse or heterogeneous data scenarios.

Overall, our proposed framework provides a statistically rigorous and computationally feasible tool for analyzing complex functional data with excess zeros and measurement error, with broad applicability in public health and behavioral science.

References

ActiGraph. GT3X+ and wGT3X+ Device Manual, 2013. URL <http://s3.amazonaws.com/actigraphcorp.com/wp-content/uploads/2018/02/22094126/GT3X-wGT3X-Device-Manual-110315.pdf>. Accessed: 2025-10-01.

Greg Atkinson and Alan M Nevill. Statistical methods for assessing measurement error (reliability) in variables relevant to sports medicine. *Sports Medicine*, 26:217–238, 1998.

Makoto Ayabe, Hideaki Kumahara, Kazuhiro Morimura, and Hiroaki Tanaka. Epoch length and the physical activity bout analysis: an accelerometry research issue. *BMC Research Notes*, 6:1–7, 2013.

David R Bassett Jr, Ann V Rowlands, and Stewart G Trost. Calibration and validation of wearable monitors. *Medicine and Science in Sports and Exercise*, 44(1 Suppl 1):S32, 2012.

Mark E Benden, Jamilia J Blake, Monica L Wendel, and John C Huber Jr. The impact of stand-biased desks in classrooms on calorie expenditure in children. *American Journal of Public Health*, 101(8):1433–1436, 2011.

Mark E Benden, Hongwei Zhao, Christina E Jeffrey, Monica L Wendel, and Jamilia J Blake. The evaluation of the impact of a stand-biased desk on energy expenditure and physical activity for elementary school students. *International Journal of Environmental Research and Public Health*, 11(9):9361–9375, 2014.

Denis Bosq. *Linear Processes in Function Spaces: Theory and Applications*, volume 149 of *Lecture Notes in Statistics*. Springer Science + Business Media, New York, New York, USA, 2000.

Jennifer A Bunn, James W Navalta, Charles J Fountaine, and JOEL D REECE. Current state of commercial wearable technology in physical activity monitoring 2015–2017. *International Journal of Exercise Science*, 11(7):503, 2018.

Nancy F Butte, Ulf Ekelund, and Klaas R Westerterp. Assessing physical activity using wearable monitors: measures of physical activity. *Medicine and Science in Sports and Exercise*, 44(1 Suppl 1):S5–S12, 2012.

Harlan Campbell. The consequences of checking for zero-inflation and overdispersion in the analysis of count data. *Methods in Ecology and Evolution*, 12(4):665–680, 2021.

Hervé Cardot, David Degras, and Etienne Josserand. Confidence bands for Horvitz–Thompson estimators using sampled noisy functional data. *Bernoulli*, 19(5A):2067–2097, Nov 2013. doi: 10.3150/12-BEJ443.

Raymond J. Carroll, David Ruppert, and Leonard A. Stefanski. *Measurement Error in Nonlinear Models*, volume 105. CRC Press, Boca Raton, Florida, USA, 1995.

Raymond J. Carroll, David Ruppert, Leonard A. Stefanski, and Ciprian M. Crainiceanu. *Measurement Error in Nonlinear Models: A Modern Perspective*. Chapman and Hall/CRC, Boca Raton, Florida, USA, 2006.

Carl J Caspersen, Kenneth E Powell, and Gregory M Christenson. Physical activity, exercise, and physical fitness: definitions and distinctions for health-related research. *Public Health Reports*, 100(2):126, 1985.

Centers for Disease Control and Prevention (CDC). QuickStats: Prevalence of obesity and severe obesity among persons aged 2–19 years — national health and nutrition examination survey, 1999–2000 through 2017–2018. *MMWR Morbidity and Mortality Weekly Report*, 69:390, 2020. doi: 10.15585/mmwr.mm6913a6.

Centers for Disease Control and Prevention, National Center for Health Statistics. National health and nutrition examination survey 2013–2014 data documentation, codebook, and frequencies physical activity monitor - minute (PAXMIN_H), 2020. URL https://www.cdc.gov/Nchs/Nhanes/2013-2014/PAXMIN_H.htm. Accessed: 2024-10-01.

Shein-Chung Chow. *Advanced Linear Models: Theory and Applications*. Routledge, New York, New York, USA, 2018.

Kirsten Corder, Søren Brage, and Ulf Ekelund. Accelerometers and pedometers: methodology and clinical application. *Current Opinion in Clinical Nutrition & Metabolic Care*, 10(5):597–603, 2007.

Steven S Coughlin and Jessica Stewart. Use of consumer wearable devices to promote physical activity: a review of health intervention studies. *Journal of Environment and Health Sciences*, 2 (6), 2016.

Ciprian M. Crainiceanu, Jeff Goldsmith, Andrew Leroux, and Erjia Cui. *Functional Data Analysis with R*. CRC Press, Boca Raton, Florida, USA, 2024.

Christophe Crambes, Alois Kneip, and Pascal Sarda. Smoothing spline estimators for functional linear regression. *The Annals of Statistics*, 37(1):35–72, 2009.

Erjia Cui, Andrew Leroux, Ekaterina Smirnova, and Ciprian M Crainiceanu. Fast univariate inference for longitudinal functional models. *Journal of Computational and Graphical Statistics*, 31(1):219–230, 2022.

Massimiliano De Zambotti, Nicola Cellini, Aimee Goldstone, Ian M Colrain, and Fiona C Baker. Wearable sleep technology in clinical and research settings. *Medicine and Science in Sports and Exercise*, 51(7):1538, 2019.

William H Dietz. Childhood weight affects adult morbidity and mortality. *The Journal of Nutrition*, 128(2):411S–414S, 1998.

Mahyar Etminan, James M Brophy, Gary Collins, Maryam Nazemipour, and Mohammad Ali Mansournia. To adjust or not to adjust: the role of different covariates in cardiovascular observational studies. *American Heart Journal*, 237:62–67, 2021.

Lynne M Feehan, Jasmina Geldman, Eric C Sayre, Chance Park, Allison M Ezzat, Ju Young Yoo, Clayton B Hamilton, and Linda C Li. Accuracy of Fitbit devices: systematic review and narrative syntheses of quantitative data. *JMIR mHealth and uHealth*, 6(8):e10527, 2018.

Pietro Ferrari, Christine Friedenreich, and Charles E Matthews. The role of measurement error in estimating levels of physical activity. *American Journal of Epidemiology*, 166(7):832–840, 2007.

Frédéric Ferraty and Philippe Vieu. *Nonparametric Functional Data Analysis: Theory and Practice*. Springer, New York, New York, USA, 2006.

Jean-Pierre Florens and Sébastien Van Bellegem. Instrumental variable estimation in functional linear models. *Journal of Econometrics*, 186(2):465–476, 2015.

Stephen H Friend, Geoffrey S Ginsburg, and Rosalind W Picard. Wearable digital health technology, 2023.

Wayne A. Fuller. *Measurement Error Models*. John Wiley & Sons, Hoboken, New Jersey, USA, 2009.

Jan Gertheiss, David Rügamer, Bernard XW Liew, and Sonja Greven. Functional data analysis: An introduction and recent developments. *Biometrical Journal*, 66(7):e202300363, 2024.

Juvenile Diabetes Research Foundation Continuous Glucose Monitoring Study Group. Continuous glucose monitoring and intensive treatment of type 1 diabetes. *New England Journal of Medicine*, 359(14):1464–1476, 2008.

Peter Hall and Mohammad Hosseini-Nasab. On properties of functional principal components analysis. *Journal of the Royal Statistical Society Series B: Statistical Methodology*, 68(1):109–126, 2006.

Peter Hall, Hans-Georg Müller, and Jane-Ling Wang. Properties of principal component methods for functional and longitudinal data analysis. *The Annals of Statistics*, 34(3):1493–1517, 2006. doi: 10.1214/009053606000000272.

James W Hardin, Henrik Schmiediche, and Raymond J Carroll. The regression-calibration method for fitting generalized linear models with additive measurement error. *The Stata Journal*, 3(4):361–372, 2003.

Qi-Fang Huang, Wen-Yi Yang, Kei Asayama, Zhen-Yu Zhang, Lutgarde Thijs, Yan Li, Eoin O'Brien, and Jan A Staessen. Ambulatory blood pressure monitoring to diagnose and manage hypertension. *Hypertension*, 77(2):254–264, 2021.

Cuiqiong Huo, Yuanyuan Luan, Roger S Zoh, Nana Gletsu-Miller, Stephen J Carter, Georgia Frey, Hsien-Chang Lin, Aurelian Bidulescu, See Ling Loy, Marwah Abdalla, et al. Comparison of two measurement error–correction approaches for assessing the association between choline intake and coronary heart disease prevalence among us community-dwelling adults. *Annals of Epidemiology*, 2025.

Sneha Jadhav, Carmen D Tekwe, and Yuanyuan Luan. A function-based approach to model the measurement error in wearable devices. *Statistics in Medicine*, 41(24):4886–4902, 2022.

Renee M Jeffries, Thomas H Inge, Todd M Jenkins, Wendy King, Vedran Oruc, Andrew D Douglas, and Molly Bray. Physical activity monitoring in extremely obese adolescents from the Teen-LABS study. *Journal of Physical Activity & Health*, 12(1):132, 2014.

Heyang Ji, Ufuk Beyaztas, Yuanyuan Luan, Xiwei Chen, Mengli Zhang, Roger Zoh, Lan Xue, and Carmen Tekwe. *MECfda: Scalar-on-Function Regression with Measurement Error Correction*, 2025. URL <https://CRAN.R-project.org/package=MECfda>. R package version 0.2.0.

David C Klonoff. Continuous glucose monitoring: roadmap for 21st century diabetes therapy. *Diabetes Care*, 28(5):1231–1239, 2005.

David C Klonoff, David Ahn, and Andjela Drincic. Continuous glucose monitoring: a review of the technology and clinical use. *Diabetes Research and Clinical Practice*, 133:178–192, 2017.

Sarah L Kozey, Kate Lyden, Cheryl A Howe, John W Staudenmayer, and Patty S Freedson. Accelerometer output and MET values of common physical activities. *Medicine & Science in Sports & Exercise*, 42(9):1776, 2010.

Diane Lambert. Zero-inflated Poisson regression, with an application to defects in manufacturing. *Technometrics*, 34(1):1–14, 1992.

Andy H Lee, Yun Zhao, Kelvin KW Yau, and Liming Xiang. How to analyze longitudinal multilevel physical activity data with many zeros? *Preventive Medicine*, 51(6):476–481, 2010.

Liang Li, Jun Shao, and Mari Palta. A longitudinal measurement error model with a semicontinuous covariate. *Biometrics*, 61(3):824–830, 2005.

Yuanyuan Luan, Roger S Zoh, Erjia Cui, Xue Lan, Sneha Jadhav, and Carmen D Tekwe. Scalable regression calibration approaches to correcting measurement error in multi-level generalized functional linear regression models with heteroscedastic measurement errors. *arXiv Preprint Arxiv:2305.12624*, 2023.

John J Mastrototaro. The MiniMed continuous glucose monitoring system. *Diabetes Technology & Therapeutics*, 2(1, Supplement 1):13–18, 2000.

Charles E Matthews, Kong Y Chen, Patty S Freedson, Maciej S Buchowski, Bettina M Beech, Russell R Pate, and Richard P Troiano. Amount of time spent in sedentary behaviors in the United States, 2003–2004. *American Journal of Epidemiology*, 167(7):875–881, 2008.

Charles E McCulloch and John M Neuhaus. Prediction of random effects in linear and generalized linear models under model misspecification. *Biometrics*, 67(1):270–279, 2011.

Daniel J McDonough, Xiwen Su, and Zan Gao. Health wearable devices for weight and bmi reduction in individuals with overweight/obesity and chronic comorbidities: systematic review and network meta-analysis. *British Journal of Sports Medicine*, 55(16):917–925, 2021.

Elizabeth Dastrup Mills. *Adjusting for Covariates in Zero-Inflated Gamma and Zero-Inflated Log-Normal Models for Semicontinuous Data*. The University of Iowa, Iowa City, Iowa, USA, 2013.

Jeffrey S Morris. Functional regression. *Annual Review of Statistics and Its Application*, 2(1):321–359, 2015.

Tim P Morris, A Sarah Walker, Elizabeth J Williamson, and Ian R White. Planning a method for covariate adjustment in individually randomised trials: a practical guide. *Trials*, 23(1):328, 2022.

Hans-Olof Mossberg. 40-year follow-up of overweight children. *The Lancet*, 334(8661):491–493, 1989.

Amir Muaremi, Bert Arnrich, and Gerhard Tröster. Towards measuring stress with smartphones and wearable devices during workday and sleep. *Bionanoscience*, 3:172–183, 2013.

Hans-Georg Müller and Ulrich Stadtmüller. Generalized functional linear models. *The Annals of Statistics*, 33(2):774–805, 2005. doi: 10.1214/009053604000001156.

Aline Araújo Nobre, Marilia Sá Carvalho, Rosane Härter Griep, Maria de Jesus Mendes da Fonseca, Enirtes Caetano Prates Melo, Itamar de Souza Santos, and Dora Chor. Multinomial model and zero-inflated gamma model to study time spent on leisure time physical activity: an example of ELSA-Brasil. *Revista de Saúde Pública*, 51:76, 2017.

Eoin O'Brien, William B White, Gianfranco Parati, and Eamon Dolan. Ambulatory blood pressure monitoring in the 21st century. *the Journal of Clinical Hypertension*, 20(7):1108–1111, 2018.

Siobhan M Phillips, Lisa Cadmus-Bertram, Dori Rosenberg, Matthew P Buman, and Brigid M Lynch. Wearable technology and physical activity in chronic disease: opportunities and challenges. *American Journal of Preventive Medicine*, 54(1):144–150, 2018.

Thomas Pickering. Recommendations for the use of home (self) and ambulatory blood pressure monitoring. *American Journal of Hypertension*, 9(1):1–11, 1996.

Thomas G Pickering, Daichi Shimbo, and Donald Haas. Ambulatory blood-pressure monitoring. *New England Journal of Medicine*, 354(22):2368–2374, 2006.

Guy Plasqui and Klaas R Westerterp. Physical activity assessment with accelerometers: an evaluation against doubly labeled water. *Obesity*, 15(10):2371–2379, 2007.

Guy Plasqui, Alberto G Bonomi, and Klaas R Westerterp. Daily physical activity assessment with accelerometers: new insights and validation studies. *Obesity Reviews*, 14(6):451–462, 2013.

James Ramsay, Giles Hooker, Spencer Graves, JO Ramsay, Giles Hooker, and Spencer Graves. Introduction to functional data analysis. *Functional Data Analysis with R and MATLAB*, pages 1–19, 2009.

James O. Ramsay and Bernard W. Silverman. *Functional Data Analysis*. Springer Series in Statistics. Springer, New York, New York, USA, 2nd edition, 2005.

Philip T Reiss, Jeff Goldsmith, Han Lin Shang, and R Todd Ogden. Methods for scalar-on-function regression. *International Statistical Review*, 85(2):228–249, 2017.

Martin Ridout, Clarice GB Demétrio, and John Hinde. Models for count data with many zeros. In *Proceedings of the XIXth international biometric conference*, volume 19, pages 179–192. International Biometric Society Invited Papers Cape Town, South Africa, 1998.

Wendy Robertson, Sarah Stewart-Brown, Elizabeth Wilcock, Michelle Oldfield, and Margaret Thorogood. Utility of accelerometers to measure physical activity in children attending an obesity treatment intervention. *Journal of Obesity*, 2011(1):398918, 2011.

David Rodbard. Continuous glucose monitoring: a review of successes, challenges, and opportunities. *Diabetes Technology & Therapeutics*, 18(S2):S2–3, 2016.

Megan P Rothney, Emily V Schaefer, Megan M Neumann, Leena Choi, and Kong Y Chen. Validity of physical activity intensity predictions by actiGraph, actical, and RT3 accelerometers. *Obesity*, 16(8):1946–1952, 2008.

Ann V Rowlands, Philip WM Thomas, Roger G Eston, and Rodney Topping. Validation of the RT3 triaxial accelerometer for the assessment of physical activity. *Medicine & Science in Sports & Exercise*, 36(3):518–524, 2004.

Charli Sargent, Michele Lastella, Georgia Romyn, Nathan Versey, Dean J Miller, and Gregory D Roach. How well does a commercially available wearable device measure sleep in young athletes? *Chronobiology International*, 35(6):754–758, 2018.

Holger Schielzeth, Niels J Dingemanse, Shinichi Nakagawa, David F Westneat, Hassen Allegue, Céline Teplitsky, Denis Réale, Ned A Dochtermann, László Zsolt Garamszegi, and Yimen G Araya-Ajoy. Robustness of linear mixed-effects models to violations of distributional assumptions. *Methods in Ecology and Evolution*, 11(9):1141–1152, 2020.

Hannah Scott, Leon Lack, and Nicole Lovato. A systematic review of the accuracy of sleep wearable devices for estimating sleep onset. *Sleep Medicine Reviews*, 49:101227, 2020.

Sijing SJ Shao, Ziqian Xu, Qimin Liu, Kenneth McClure, Ross Jacobucci, Scott E Maxwell, and Zhiyong Zhang. Zero inflation in intensive longitudinal data: why is it important and how should we deal with it? *Psychological Methods*, 2025.

Mark Simmonds, Alexis Llewellyn, Christopher G Owen, and Nerys Woolacott. Predicting adult obesity from childhood obesity: a systematic review and meta-analysis. *Obesity Reviews*, 17(2): 95–107, 2016.

Donna Spiegelman, Aidan McDermott, and Bernard Rosner. Regression calibration method for correcting measurement-error bias in nutritional epidemiology. *The American Journal of Clinical Nutrition*, 65(4):1179S–1186S, 1997.

Tessa Strain, Katrien Wijndaele, Paddy C Dempsey, Stephen J Sharp, Matthew Pearce, Justin Jeon, Tim Lindsay, Nick Wareham, and Søren Brage. Wearable-device-measured physical activity and future health risk. *Nature Medicine*, 26(9):1385–1391, 2020.

Megan K Tait, Julie Horrocks, and Kathleen A Martin Ginis. Modelling longitudinal count data with zero-inflation: An application to physical activity. *Journal of Statistics and Applications*, 7 (1/2):55, 2012.

Eduardo Teixeira, Hélder Fonseca, Florêncio Diniz-Sousa, Lucas Veras, Giorjines Boppre, José Oliveira, Diogo Pinto, Alberto Jorge Alves, Ana Barbosa, Romeu Mendes, et al. Wearable devices for physical activity and healthcare monitoring in elderly people: A critical review. *Geriatrics*, 6 (2):38, 2021.

Carmen D Tekwe, Mengli Zhang, Raymond J Carroll, Yuanyuan Luan, Lan Xue, Roger S Zoh, Stephen J Carter, David B Allison, and Marco Geraci. Estimation of sparse functional quantile regression with measurement error: a SIMEX approach. *Biostatistics*, 23(4):1218–1241, 2022.

Selene Y Tobin, Paula G Williams, Kelly G Baron, Tanya M Halliday, and Christopher M Depner. Challenges and opportunities for applying wearable technology to sleep. *Sleep Medicine Clinics*, 16(4):607–618, 2021.

Janet A Tooze, Gary K Grunwald, and Richard H Jones. Analysis of repeated measures data with clumping at zero. *Statistical Methods in Medical Research*, 11(4):341–355, 2002.

Richard P Troiano. Evolution of public health physical activity applications of accelerometers: A personal perspective. *Journal for the Measurement of Physical Behaviour*, 6(1):13–18, 2023.

Richard P Troiano, David Berrigan, Kevin W Dodd, Louise C Masse, Timothy Tilert, Margaret McDowell, et al. Physical activity in the United States measured by accelerometer. *Medicine and Science in Sports and Exercise*, 40(1):181, 2008.

Wanzhu Tu. Zero-inflated data. *Encyclopedia of Environmetrics*, 2006.

J Rick Turner, Anthony J Viera, and Daichi Shimbo. Ambulatory blood pressure monitoring in clinical practice: a review. *the American Journal of Medicine*, 128(1):14–20, 2015.

Shahid Ullah and Caroline F Finch. Applications of functional data analysis: A systematic review. *BMC Medical Research Methodology*, 13:1–12, 2013.

Ching-Yun Wang, Jean de Dieu Tapsoba, Catherine Duggan, and Anne McTiernan. Generalized linear models with covariate measurement error and zero-inflated surrogates. *Mathematics*, 12(2):309, 2024.

CY Wang, Li Hsu, ZD Feng, and Ross L Prentice. Regression calibration in failure time regression. *Biometrics*, pages 131–145, 1997.

Jane-Ling Wang, Jeng-Min Chiou, and Hans-Georg Müller. Functional data analysis. *Annual Review of Statistics and Its Application*, 3(1):257–295, 2016.

Wentao Wang, Jing Cheng, Weijun Song, Yi Shen, et al. The effectiveness of wearable devices as physical activity interventions for preventing and treating obesity in children and adolescents: systematic review and meta-analysis. *JMIR mHealth and uHealth*, 10(4):e32435, 2022.

Monica L Wendel, Mark E Benden, Hongwei Zhao, and Christina Jeffrey. Stand-biased versus seated classrooms and childhood obesity: a randomized experiment in Texas. *American Journal of Public Health*, 106(10):1849–1854, 2016.

World Health Organization. *Global Action Plan on Physical Activity 2018–2030: More Active People for a Healthier World*. World Health Organization, Geneva, Switzerland, 2019.

Xianhong Xie, Xiaonan Xue, and Howard D Strickler. Generalized linear mixed model for binary outcomes when covariates are subject to measurement errors and detection limits. *Statistics in Medicine*, 37(1):119–136, 2018.

Fang Yao, Hans-Georg Müller, and Jane-Ling Wang. Functional data analysis for sparse longitudinal data. *Journal of the American Statistical Association*, 100(470):577–590, 2005.

Mengli Zhang, Lan Xue, Carmen D Tekwe, Yang Bai, and Annie Qu. Partially functional linear quantile regression with measurement errors. *Statistica Sinica*, 33(3):2257, 2023.

Roger S Zoh, Yuanyuan Luan, Lan Xue, David B Allison, and Carmen D Tekwe. A Bayesian semi-parametric scalar-on-function regression with measurement error using instrumental variables. *Statistics in Medicine*, 43(21):4043–4054, 2024.

Appendix A Notations

Here we provide the definition of some notations used in Lemma 1 and Theorem 2.

- For an element in $L^2(\Omega)$, $\|\cdot\|_{L^2(\Omega)}$ denotes the L^2 norm on Ω , i.e., $\|\beta\|_{L^2(\Omega)} = \left(\int_{\Omega} |\beta(t)|^2 dt\right)^{1/2}$, abbreviated as $\|\cdot\|_{L^2}$ when the domain is clear.
- For a measureable subset of \mathbb{R} , $\|\Omega\|$ denotes the Lebesgue measure of Ω , i.e., $\|\Omega\| = \int_{\Omega} 1 dt$.
- For a finite set \mathcal{T} , $|\mathcal{T}|$ denotes its cardinality; e.g., if $\mathcal{T} = \{t_1, \dots, t_m\}$ then $|\mathcal{T}| = m$.
- Let $\beta_K(t) = \sum_{k=1}^K b_k \rho_k(t)$ denote the approximation of β onto the first K basis functions.

Appendix B Proofs

Appendix B.1 Auxiliary Lemmas

Before proving the main results we collect two auxiliary facts.

Lemma 3. *Let X be a random variable and, conditional on X , let W_1, \dots, W_J be i.i.d. copies of a proxy variable W . Suppose that*

- (E1) $W_j | X = x \stackrel{\text{i.i.d.}}{\sim} F_{W|X}(\cdot | x)$;
- (E2) for any $x_1 \neq x_2$, $F_{W|X=x_1} \neq F_{W|X=x_2}$ (identifiability);
- (E3) for any j , $\text{Var}(W_j | X) < \infty$.

Then

$$\mathbb{E}[X | \widehat{W}] \xrightarrow{a.s.} X \quad (J \rightarrow \infty), \quad \text{where } \widehat{W} := (W_1, \dots, W_J)^\top.$$

This Lemma 3 is also a well known result. It shows that the conditional expectation of X given a large number of i.i.d. observations of W (if conditional on X) converges to X almost surely, under certain conditions. Its proof is omitted.

Lemma 4. *Let*

$$h(Z) = (Z^\top Z)^{-1} Z y, \quad Z \in \mathbb{R}^{n \times p}, y \in \mathbb{R}^n.$$

Suppose $\{Z_1^{(m)}\}_{m \geq 1}$ and Z_2 are design matrices with identical dimensions such that

$$Z_1^{(m)} \xrightarrow{P} Z_2 \quad (\text{element-wise, equivalently } \|Z_1^{(m)} - Z_2\|_F \xrightarrow{P} 0).$$

If $Z_2^\top Z_2$ is invertible (i.e. $\lambda_{\min}(Z_2^\top Z_2) > 0$), then

$$h(Z_1^{(m)}) \xrightarrow{P} h(Z_2).$$

Proof of Lemma 4. For any matrices A, B of the same size,

$$\|A^\top A - B^\top B\|_F \leq \|A^\top (A - B)\|_F + \|(A - B)^\top B\|_F \leq (\|A\|_F + \|B\|_F) \|A - B\|_F.$$

Hence $\|Z_1^{(m)\top} Z_1^{(m)} - Z_2^\top Z_2\|_F \xrightarrow{P} 0$. Write $A_m = Z_1^{(m)\top} Z_1^{(m)}$ and $A = Z_2^\top Z_2$. Weyl's inequality yields

$$|\lambda_{\min}(A_m) - \lambda_{\min}(A)| \leq \|A_m - A\|_2 \leq \|A_m - A\|_F \xrightarrow{P} 0.$$

Because $\lambda_{\min}(A) > 0$, it follows that $\lambda_{\min}(A_m) \xrightarrow{P} \lambda_{\min}(A) > 0$, so A_m is invertible with probability tending to one and $A_m^{-1} \xrightarrow{P} A^{-1}$. The matrix inversion map is continuous on the set of invertible matrices, and matrix multiplication is jointly continuous. Consequently,

$$(Z_1^{(m)\top} Z_1^{(m)})^{-1} \xrightarrow{P} (Z_2^\top Z_2)^{-1}, \quad Z_1^{(m)} \xrightarrow{P} Z_2.$$

Slutsky's theorem therefore gives

$$(Z_1^{(m)\top} Z_1^{(m)})^{-1} Z_1^{(m)} \xrightarrow{P} (Z_2^\top Z_2)^{-1} Z_2.$$

If y is deterministic (or independent of the $Z_1^{(m)}$ sequence with finite second moment), another application of Slutsky yields

$$h(Z_1^{(m)}) = (Z_1^{(m)\top} Z_1^{(m)})^{-1} Z_1^{(m)} y \xrightarrow{P} (Z_2^\top Z_2)^{-1} Z_2 y = h(Z_2).$$

□

Appendix B.2 Proof of Theorem 2

Proof of Theorem 2. We decompose the estimation error using the triangle inequality,

$$\|\widehat{\beta}_{K_n} - \beta\|_{L^2(\Omega)} \leq \|\widetilde{\beta}_{K_n} - \widehat{\beta}_{K_n}\|_{L^2(\Omega)} + \|\widetilde{\beta}_{K_n} - \beta\|_{L^2(\Omega)}. \quad (12)$$

Based on the Lemma 1, we already have $\|\widetilde{\beta}_{K_n} - \beta\|_{L^2(\Omega)} \xrightarrow{P} 0$ as $n \rightarrow \infty$. Therefore, we only need to show $\|\widehat{\beta}_{K_n} - \widetilde{\beta}_{K_n}\|_{L^2(\Omega)} \xrightarrow{P} 0$, equivalently, $\|\widehat{\theta}_{K_n} - \widetilde{\theta}_{K_n}\| \xrightarrow{P} 0$.

Let $\mathbf{y} := (Y_1, \dots, Y_n)^\top$ be the vector of response. And the least-squares estimator $\widehat{\theta}_{K_n}$ and $\widetilde{\theta}_{K_n}$ can be expressed in closed form of $\widehat{\theta}_{K_n} = (\widehat{\mathbf{X}}_{K_n}^\top \widehat{\mathbf{X}}_{K_n})^{-1} \widehat{\mathbf{X}}_{K_n}^\top \mathbf{y}$ and $\widetilde{\theta}_{K_n} = (\mathbf{X}_{K_n}^\top \mathbf{X}_{K_n})^{-1} \mathbf{X}_{K_n}^\top \mathbf{y}$.

Because \mathbf{X}_{K_n} and $\widehat{\mathbf{X}}_{K_n}$ have full column rank, $\mathbf{X}_{K_n}^\top \mathbf{X}_{K_n}$ and $\widehat{\mathbf{X}}_{K_n}^\top \widehat{\mathbf{X}}_{K_n}$ are both invertable. Based on Lemma 4, to show $\|\widehat{\beta}_{K_n} - \widetilde{\beta}_{K_n}\|_{L^2(\Omega)} \xrightarrow{P} 0$, we only need to show that $|\widehat{x}_{ik} - x_{ik}| \xrightarrow{P} 0$, equivalently $\frac{\|\Omega\|}{|\mathcal{T}_m|} \sum_{t \in \mathcal{T}_m} \widehat{X}_i(t) \rho_k(t) \rightarrow \int_{\Omega} X_i(t) \rho_k(t) dt$.

We decompose $|\widehat{x}_{ik} - x_{ik}|$ as follows:

$$|\widehat{x}_{ik} - x_{ik}| \leq |\widehat{x}_{ik} - A_m| + |A_m - x_{ik}|$$

where $A_m = \frac{\|\Omega\|}{|\mathcal{T}_m|} \sum_{t \in \mathcal{T}_m} X_i(t) \rho_k(t)$.

Since

$$\widehat{x}_{ik} - A_m = \frac{\|\Omega\|}{|\mathcal{T}_m|} \sum_{t \in \mathcal{T}_m} \{X_i(t) - \widehat{X}_i(t)\} \rho_k(t),$$

and we have $\widehat{X}_i(t) \xrightarrow{a.s.} X_i(t)$ as $J_i \rightarrow \infty$ for any i and t (by Lemma 3), the first term $|\widehat{x}_{ik} - A_m|$ can be shown to converge to 0 as $J_i \rightarrow \infty$ for any i and k .

The second term $|A_m - x_{ik}|$ can be proven to converge to 0 as $\Delta_m \rightarrow 0$ by Riemann-Lebesgue Theorem.

Combining the pieces, we have

$$\|\widehat{\beta}_{K_n} - \beta\|_{L^2(\Omega)} \xrightarrow{P} 0$$

as $n \rightarrow \infty$, $\inf_i J_i \rightarrow \infty$, and $m \rightarrow \infty$.

□

(Undefined notation is summarized in Section [Appendix A](#).)

Appendix C Simulation Results

In the main text (Section 3.2), we presented selected results from the simulation study under a single set of simulation settings. In this appendix, we provide additional tables that summarize the results under a wider range of settings.

Each table isolates the effect of one simulation parameter by varying it while keeping all other settings fixed. Within each table, subtable (a) reports the squared bias, and subtable (b) reports the variance of the estimator $\widehat{\beta}(t)$. For each scenario, we report the bias and variance of the estimator $\widehat{\beta}(t)$ to illustrate the impact of the specific setting on estimation performance.

Table 2: Effect of sample size. Common settings: conditional distribution of $Y|X(t), Z$: Gaussian distribution (with identity link); estimation method of $\theta(t)$: point-wise; proportion of zero values: $\mathbb{E}\{\Pr(W_{ij}(t) = 0)\} = 0.335$; Covariance function of $U(t)$: squared-exponential with $\rho_u = 0.2$; $\sigma_u = 1$; $q_g = 0$. Benchmark = benchmark method; Average = naïve average method; MM = mixed model based method proposed in Section 2.2; RC = regression calibration method proposed in Section 2.2; Non-ZI MM = non-zero-inflated mixed model based method; 1 day = naive one-day method.

(a) Squared Bias

N	Benchmark	MM	RC	Average	Non-ZI MM	1 day	basis function
50	0.0001213	0.003945	0.005530	0.1497	0.2995	0.3897	Bspline
100	0.0000903	0.003446	0.005038	0.1445	0.1689	0.3822	Bspline
200	0.0001204	0.003259	0.005246	0.1489	0.1318	0.3840	Bspline
500	0.0001262	0.002772	0.004994	0.1468	0.1190	0.3842	Bspline
1000	0.0001110	0.002619	0.004417	0.1494	0.1225	0.3846	Bspline
2000	0.0001118	0.002687	0.004671	0.1491	0.1155	0.3844	Bspline
5000	0.0001117	0.002562	0.004822	0.1485	0.1143	0.3845	Bspline
50	0.1074799	0.018802	0.011150	0.1407	0.3793	0.3897	Fourier
100	0.0128407	0.010145	0.010521	0.1378	0.1869	0.3822	Fourier
200	0.0192103	0.005523	0.006574	0.1417	0.1385	0.3840	Fourier
500	0.0070227	0.006152	0.008074	0.1397	0.1215	0.3842	Fourier
1000	0.0001395	0.003398	0.005739	0.1422	0.1261	0.3846	Fourier
2000	0.0004761	0.004042	0.006083	0.1420	0.1187	0.3844	Fourier
5000	0.0005231	0.003902	0.006130	0.1414	0.1163	0.3845	Fourier

(b) Variance

N	Benchmark	MM	RC	Average	Non-ZI MM	1 day	basis function
50	0.0023843	0.135181	0.120203	0.0586	2.6930	0.0190	Bspline
100	0.0010200	0.061922	0.049800	0.0269	0.3297	0.0085	Bspline
200	0.0005190	0.034514	0.026972	0.0155	0.1311	0.0047	Bspline
500	0.0002088	0.014465	0.010488	0.0069	0.0479	0.0018	Bspline
1000	0.0000995	0.008700	0.005136	0.0046	0.0246	0.0010	Bspline
2000	0.0000490	0.005206	0.003023	0.0033	0.0141	0.0007	Bspline
5000	0.00000199	0.004210	0.001821	0.0026	0.0085	0.0004	Bspline
50	21.7150811	1.887667	1.827130	0.3901	7.8791	0.0190	Fourier
100	8.9110659	0.798691	0.758550	0.1662	1.5090	0.0085	Fourier
200	3.9275922	0.419874	0.352485	0.0775	0.5864	0.0047	Fourier
500	1.5453553	0.171680	0.135424	0.0322	0.2068	0.0018	Fourier
1000	0.7198404	0.099063	0.071089	0.0169	0.0987	0.0010	Fourier
2000	0.3458503	0.056823	0.037739	0.0105	0.0552	0.0007	Fourier
5000	0.1465289	0.032680	0.018335	0.0065	0.0283	0.0004	Fourier

Table 3: Effect of deviation of U. Common settings: conditional distribution of $Y|X(t), Z$: Gaussian distribution (with identity link); estimation method of $\theta(t)$: point-wise; sample size: $n = 100$; proportion of zero values: $\mathbb{E}\{\Pr(W_{ij}(t) = 0)\} = 0.335$; Covariance function of $U(t)$: squared-exponential with $\rho_u = 0.2$; $q_g = 0$. Benchmark = benchmark method; Average = naïve average method; MM = mixed model based method proposed in Section 2.2; RC = regression calibration method proposed in Section 2.2; Non-ZI MM = non-zero-inflated mixed model based method; 1 day = naive one-day method.

(a) Squared Bias

σ_u	Benchmark	MM	RC	Average	Non-ZI MM	1 day	basis function
1	0.0000903	0.003446	0.005038	0.1445	0.1689	0.3822	Bspline
2	0.0000903	0.014637	0.023435	0.1913	0.2151	0.4180	Bspline
3	0.0000903	0.033851	0.076080	0.2534	1117.2726	0.4461	Bspline
1	0.0128407	0.010145	0.010521	0.1378	0.1869	0.3822	Fourier
2	0.0128407	0.025381	0.028824	0.1866	0.2678	0.4180	Fourier
3	0.0128407	0.081917	0.077106	0.2517	1.8979	0.4461	Fourier

(b) Variance

σ_u	Benchmark	MM	RC	Average	Non-ZI MM	1 day	basis function
1	0.001020	0.061922	0.049800	0.0269	0.3297	0.0085	Bspline
2	0.001020	0.187533	0.100191	0.0262	1.0378	0.0068	Bspline
3	0.001020	0.571430	0.114888	0.0236	544845.5255	0.0052	Bspline
1	8.911066	0.798691	0.758550	0.1662	1.5090	0.0085	Fourier
2	8.911066	1.574898	0.926606	0.1670	3.9490	0.0068	Fourier
3	8.911066	8.294103	0.842241	0.1484	168.2378	0.0052	Fourier

Table 4: Effect of correlation of u . Common settings: conditional distribution of $Y|X(t), Z$: Gaussian distribution (with identity link); estimation method of $\theta(t)$: point-wise; sample size: $n = 100$; proportion of zero values: $\mathbb{E}\{\Pr(W_{ij}(t) = 0)\} = 0.335$; $\sigma_u = 1$; $q_g = 0$. Benchmark = benchmark method; Average = naïve average method; MM = mixed model based method proposed in Section 2.2; RC = regression calibration method proposed in Section 2.2; Non-ZI MM = non-zero-inflated mixed model based method; 1 day = naive one-day method.

(a) Squared Bias

correlation function U	ρ_u	Benchmark	MM	RC	Average	Non-ZI MM	1 day	basis function
AR1	0.20	0.0000903	0.011834	0.008028	0.1305	0.2135	0.3678	Bspline
AR1	0.40	0.0000903	0.009961	0.006499	0.1323	0.2004	0.3697	Bspline
AR1	0.60	0.0000903	0.007081	0.004566	0.1361	0.1959	0.3734	Bspline
Compound symmetry	0.20	0.0000903	0.013329	0.009169	0.1295	0.2217	0.3664	Bspline
Compound symmetry	0.40	0.0000903	0.013075	0.008865	0.1302	0.2255	0.3662	Bspline
Compound symmetry	0.60	0.0000903	0.012792	0.008586	0.1304	0.2263	0.3670	Bspline
Squared Exponential	0.10	0.0000903	0.005598	0.004456	0.1427	0.1840	0.3790	Bspline
Squared Exponential	0.15	0.0000903	0.003775	0.003768	0.1448	0.1764	0.3812	Bspline
Squared Exponential	0.20	0.0000903	0.003446	0.005038	0.1445	0.1689	0.3822	Bspline
AR1	0.20	0.0128407	0.011961	0.008230	0.1233	0.2384	0.3678	Fourier
AR1	0.40	0.0128407	0.009733	0.006574	0.1241	0.2179	0.3697	Fourier
AR1	0.60	0.0128407	0.006987	0.005004	0.1282	0.2117	0.3734	Fourier
Compound symmetry	0.20	0.0128407	0.013377	0.009305	0.1214	0.2515	0.3664	Fourier
Compound symmetry	0.40	0.0128407	0.013624	0.009515	0.1227	0.2598	0.3662	Fourier
Compound symmetry	0.60	0.0128407	0.013076	0.009213	0.1219	0.2699	0.3670	Fourier
Squared Exponential	0.10	0.0128407	0.009087	0.007798	0.1367	0.2050	0.3790	Fourier
Squared Exponential	0.15	0.0128407	0.008810	0.009966	0.1377	0.1912	0.3812	Fourier
Squared Exponential	0.20	0.0128407	0.010145	0.010521	0.1378	0.1869	0.3822	Fourier

(b) Variance

correlation function U	ρ_u	Benchmark	MM	RC	Average	Non-ZI MM	1 day	basis function
AR1	0.20	0.001020	0.021621	0.013414	0.0252	0.3825	0.0085	Bspline
AR1	0.40	0.001020	0.024735	0.016722	0.0252	0.3101	0.0083	Bspline
AR1	0.60	0.001020	0.032121	0.023158	0.0252	0.2978	0.0081	Bspline
Compound symmetry	0.20	0.001020	0.022135	0.012388	0.0259	0.3221	0.0086	Bspline
Compound symmetry	0.40	0.001020	0.024029	0.014656	0.0258	0.3433	0.0085	Bspline
Compound symmetry	0.60	0.001020	0.027675	0.017451	0.0261	0.3292	0.0088	Bspline
Squared Exponential	0.10	0.001020	0.036727	0.030305	0.0255	0.3730	0.0080	Bspline
Squared Exponential	0.15	0.001020	0.052211	0.043760	0.0262	0.3314	0.0084	Bspline
Squared Exponential	0.20	0.001020	0.061922	0.049800	0.0269	0.3297	0.0085	Bspline
AR1	0.20	8.911066	0.095675	0.066729	0.1245	1.2455	0.0085	Fourier
AR1	0.40	8.911066	0.122368	0.092885	0.1246	1.2295	0.0083	Fourier
AR1	0.60	8.911066	0.174827	0.141824	0.1297	1.2172	0.0081	Fourier
Compound symmetry	0.20	8.911066	0.114145	0.070892	0.1298	1.5421	0.0086	Fourier
Compound symmetry	0.40	8.911066	0.134355	0.090184	0.1370	1.6842	0.0085	Fourier
Compound symmetry	0.60	8.911066	0.172675	0.126338	0.1428	2.5201	0.0088	Fourier
Squared Exponential	0.10	8.911066	0.364757	0.330020	0.1482	1.3609	0.0080	Fourier
Squared Exponential	0.15	8.911066	0.694774	0.643891	0.1638	1.4703	0.0084	Fourier
Squared Exponential	0.20	8.911066	0.798691	0.758550	0.1662	1.5090	0.0085	Fourier

Table 5: Effect of proportion of zero values in W . Common settings: conditional distribution of $Y|X(t), Z$: Gaussian distribution (with identity link); estimation method of $\theta(t)$: point-wise; sample size: $n = 100$; Covariance function of $U(t)$: squared-exponential with $\rho_u = 0.2$; $\sigma_u = 1$; $q_g = 0$. Benchmark = benchmark method; Average = naïve average method; MM = mixed model based method proposed in Section 2.2; RC = regression calibration method proposed in Section 2.2; Non-ZI MM = non-zero-inflated mixed model based method; 1 day = naive one-day method.

(a) Squared Bias							
E(PrW=0)	Benchmark	MM	RC	Average	Non-ZI MM	1 day	basis function
0.255	0.0000903	0.006718	0.007163	0.1074	0.0986	0.3451	Bspline
0.294	0.0000903	0.004593	0.005817	0.1258	0.1323	0.3641	Bspline
0.335	0.0000903	0.003446	0.005038	0.1445	0.1689	0.3822	Bspline
0.403	0.0000903	0.002542	0.003985	0.1770	0.2860	0.4056	Bspline
0.255	0.0128407	0.012092	0.011912	0.1034	0.1074	0.3451	Fourier
0.294	0.0128407	0.011797	0.011083	0.1192	0.1371	0.3641	Fourier
0.335	0.0128407	0.010145	0.010521	0.1378	0.1869	0.3822	Fourier
0.403	0.0128407	0.005073	0.008999	0.1684	0.3403	0.4056	Fourier

(b) Variance							
E(PrW=0)	Benchmark	MM	RC	Average	Non-ZI MM	1 day	basis function
0.255	0.001020	0.056255	0.050114	0.0313	0.1827	0.0120	Bspline
0.294	0.001020	0.059960	0.050266	0.0293	0.2373	0.0099	Bspline
0.335	0.001020	0.061922	0.049800	0.0269	0.3297	0.0085	Bspline
0.403	0.001020	0.075954	0.051316	0.0231	0.8235	0.0065	Bspline
0.255	8.911066	1.057866	0.993120	0.1829	0.9043	0.0120	Fourier
0.294	8.911066	0.941326	0.878270	0.1721	1.1069	0.0099	Fourier
0.335	8.911066	0.798691	0.758550	0.1662	1.5090	0.0085	Fourier
0.403	8.911066	0.641815	0.604558	0.1429	3.2846	0.0065	Fourier

Table 6: Effect of q_g for $G(t)$ in Eq (9). Common settings: conditional distribution of $Y|X(t), Z$: Gaussian distribution (with identity link); estimation method of $\theta(t)$: point-wise; sample size: $n = 100$; proportion of zero values: $\mathbb{E}\{\Pr(W_{ij}(t) = 0)\} = 0.335$; Covariance function of $U(t)$: squared-exponential with $\rho_u = 0.2$; $\sigma_u = 1$; Benchmark = benchmark method; Average = naïve average method; MM = mixed model based method proposed in Section 2.2; RC = regression calibration method proposed in Section 2.2; Non-ZI MM = non-zero-inflated mixed model based method; 1 day = naive one-day method.

(a) Squared Bias							
q_g	Benchmark	MM	RC	Average	Non-ZI MM	1 day	basis function
0.0	0.0000903	0.003446	0.005038	0.1445	0.1689	0.3822	Bspline
0.2	0.0000903	0.002033	0.004820	0.1618	0.0827	0.3818	Bspline
0.4	0.0000903	0.004155	0.004004	0.2052	0.0951	0.3820	Bspline
0.0	0.0128407	0.010145	0.010521	0.1378	0.1869	0.3822	Fourier
0.2	0.0128407	0.012550	0.016378	0.1536	0.0764	0.3818	Fourier
0.4	0.0128407	0.003063	0.008264	0.1970	0.0844	0.3820	Fourier

(b) Variance							
q_g	Benchmark	MM	RC	Average	Non-ZI MM	1 day	basis function
0.0	0.001020	0.061922	0.049800	0.0269	0.3297	0.0085	Bspline
0.2	0.001020	0.071695	0.049681	0.0256	0.1898	0.0082	Bspline
0.4	0.001020	0.095285	0.049205	0.0233	0.0789	0.0081	Bspline
0.0	8.911066	0.798691	0.758550	0.1662	1.5090	0.0085	Fourier
0.2	8.911066	0.746826	0.713728	0.1547	0.9039	0.0082	Fourier
0.4	8.911066	0.713032	0.664500	0.1687	0.5337	0.0081	Fourier

Table 7: Effect of sample size. Common settings: conditional distribution of $Y|X(t), Z$: Gaussian distribution (with identity link); smoothed point-wise; proportion of zero values: $\mathbb{E}\{\Pr(W_{ij}(t) = 0)\} = 0.335$; Covariance function of $U(t)$: squared-exponential with $\rho_u = 0.2$; $\sigma_u = 1$; $q_g = 0$. Benchmark = benchmark method; Average = naïve average method; MM = mixed model based method proposed in Section 2.2; RC = regression calibration method proposed in Section 2.2; Non-ZI MM = non-zero-inflated mixed model based method; 1 day = naive one-day method.

(a) Squared Bias

N	Benchmark	MM	RC	Average	Non-ZI MM	1 day	basis function
50	0.0001213	0.003914	0.005610	0.1497	0.2995	0.3897	Bspline
100	0.0000903	0.003400	0.005045	0.1445	0.1689	0.3822	Bspline
200	0.0001204	0.003118	0.005186	0.1489	0.1318	0.3840	Bspline
500	0.0001262	0.002646	0.004883	0.1468	0.1190	0.3842	Bspline
1000	0.0001110	0.002508	0.004310	0.1494	0.1225	0.3846	Bspline
50	0.1074799	0.017861	0.011053	0.1407	0.3793	0.3897	Fourier
100	0.0128407	0.009351	0.009639	0.1378	0.1869	0.3822	Fourier
200	0.0192103	0.005651	0.006818	0.1417	0.1385	0.3840	Fourier
500	0.0070227	0.006278	0.008148	0.1397	0.1215	0.3842	Fourier
1000	0.0001395	0.003415	0.005745	0.1422	0.1261	0.3846	Fourier

(b) Variance

N	Benchmark	MM	RC	Average	Non-ZI MM	1 day	basis function
50	0.0023843	0.135726	0.119692	0.0586	2.6930	0.0190	Bspline
100	0.0010200	0.062859	0.050002	0.0269	0.3297	0.0085	Bspline
200	0.0005190	0.034582	0.026807	0.0155	0.1311	0.0047	Bspline
500	0.0002088	0.014532	0.010509	0.0069	0.0479	0.0018	Bspline
1000	0.0000995	0.008773	0.005209	0.0046	0.0246	0.0010	Bspline
50	21.7150811	1.982048	1.896337	0.3901	7.8791	0.0190	Fourier
100	8.9110659	0.808248	0.760005	0.1662	1.5090	0.0085	Fourier
200	3.9275922	0.420307	0.355182	0.0775	0.5864	0.0047	Fourier
500	1.5453553	0.171809	0.134104	0.0322	0.2068	0.0018	Fourier
1000	0.7198404	0.099889	0.071308	0.0169	0.0987	0.0010	Fourier

Table 8: Effect of deviation of U. Common settings: conditional distribution of $Y|X(t), Z$: Gaussian distribution (with identity link); smoothed point-wise; sample size: $n = 100$; proportion of zero values: $\mathbb{E}\{\Pr(W_{ij}(t) = 0)\} = 0.335$; Covariance function of $U(t)$: squared-exponential with $\rho_u = 0.2$; $q_g = 0$. Benchmark = benchmark method; Average = naïve average method; MM = mixed model based method proposed in Section 2.2; RC = regression calibration method proposed in Section 2.2; Non-ZI MM = non-zero-inflated mixed model based method; 1 day = naive one-day method.

(a) Squared Bias

σ_u	Benchmark	MM	RC	Average	Non-ZI MM	1 day	basis function
1	0.0000903	0.003400	0.005045	0.1445	0.1689	0.3822	Bspline
2	0.0000903	0.014826	0.023468	0.1913	0.2151	0.4180	Bspline
3	0.0000903	0.034820	0.076291	0.2534	1117.2726	0.4461	Bspline
1	0.0128407	0.009351	0.009639	0.1378	0.1869	0.3822	Fourier
2	0.0128407	0.025021	0.028312	0.1866	0.2678	0.4180	Fourier
3	0.0128407	0.097736	0.077173	0.2517	1.8979	0.4461	Fourier

(b) Variance

σ_u	Benchmark	MM	RC	Average	Non-ZI MM	1 day	basis function
1	0.001020	0.062859	0.050002	0.0269	0.3297	0.0085	Bspline
2	0.001020	0.189413	0.100581	0.0262	1.0378	0.0068	Bspline
3	0.001020	0.577805	0.114981	0.0236	544845.5255	0.0052	Bspline
1	8.911066	0.808248	0.760005	0.1662	1.5090	0.0085	Fourier
2	8.911066	1.583932	0.928256	0.1670	3.9490	0.0068	Fourier
3	8.911066	9.735902	0.842110	0.1484	168.2378	0.0052	Fourier

Table 9: Effect of correlation of u . Common settings: conditional distribution of $Y|X(t), Z$: Gaussian distribution (with identity link); smoothed point-wise; sample size: $n = 100$; proportion of zero values: $\mathbb{E}\{\Pr(W_{ij}(t) = 0)\} = 0.335$; $\sigma_u = 1$; $q_g = 0$. Benchmark = benchmark method; Average = naïve average method; MM = mixed model based method proposed in Section 2.2; RC = regression calibration method proposed in Section 2.2; Non-ZI MM = non-zero-inflated mixed model based method; 1 day = naive one-day method.

(a) Squared Bias

correlation function U	ρ_u	Benchmark	MM	RC	Average	Non-ZI MM	1 day	basis function
AR1	0.20	0.0000903	0.011842	0.008007	0.1305	0.2135	0.3678	Bspline
AR1	0.40	0.0000903	0.009996	0.006483	0.1323	0.2004	0.3697	Bspline
AR1	0.60	0.0000903	0.007109	0.004566	0.1361	0.1959	0.3734	Bspline
Compound symmetry	0.20	0.0000903	0.013358	0.009150	0.1295	0.2217	0.3664	Bspline
Compound symmetry	0.40	0.0000903	0.013094	0.008834	0.1302	0.2255	0.3662	Bspline
Compound symmetry	0.60	0.0000903	0.012801	0.008557	0.1304	0.2263	0.3670	Bspline
Squared Exponential	0.10	0.0000903	0.005626	0.004464	0.1427	0.1840	0.3790	Bspline
Squared Exponential	0.15	0.0000903	0.003774	0.003764	0.1448	0.1764	0.3812	Bspline
Squared Exponential	0.20	0.0000903	0.003400	0.005045	0.1445	0.1689	0.3822	Bspline
AR1	0.20	0.0128407	0.011971	0.008180	0.1233	0.2384	0.3678	Fourier
AR1	0.40	0.0128407	0.009788	0.006552	0.1241	0.2179	0.3697	Fourier
AR1	0.60	0.0128407	0.007047	0.005011	0.1282	0.2117	0.3734	Fourier
Compound symmetry	0.20	0.0128407	0.013439	0.009299	0.1214	0.2515	0.3664	Fourier
Compound symmetry	0.40	0.0128407	0.013689	0.009518	0.1227	0.2598	0.3662	Fourier
Compound symmetry	0.60	0.0128407	0.013263	0.009373	0.1219	0.2699	0.3670	Fourier
Squared Exponential	0.10	0.0128407	0.009227	0.007960	0.1367	0.2050	0.3790	Fourier
Squared Exponential	0.15	0.0128407	0.009174	0.010184	0.1377	0.1912	0.3812	Fourier
Squared Exponential	0.20	0.0128407	0.009351	0.009639	0.1378	0.1869	0.3822	Fourier

(b) Variance

correlation function U	ρ_u	Benchmark	MM	RC	Average	Non-ZI MM	1 day	basis function
AR1	0.20	0.001020	0.021910	0.013392	0.0252	0.3825	0.0085	Bspline
AR1	0.40	0.001020	0.025064	0.016814	0.0252	0.3101	0.0083	Bspline
AR1	0.60	0.001020	0.032598	0.023383	0.0252	0.2978	0.0081	Bspline
Compound symmetry	0.20	0.001020	0.022411	0.012457	0.0259	0.3221	0.0086	Bspline
Compound symmetry	0.40	0.001020	0.024365	0.014776	0.0258	0.3433	0.0085	Bspline
Compound symmetry	0.60	0.001020	0.028158	0.017721	0.0261	0.3292	0.0088	Bspline
Squared Exponential	0.10	0.001020	0.036899	0.030264	0.0255	0.3730	0.0080	Bspline
Squared Exponential	0.15	0.001020	0.052564	0.043696	0.0262	0.3314	0.0084	Bspline
Squared Exponential	0.20	0.001020	0.062859	0.050002	0.0269	0.3297	0.0085	Bspline
AR1	0.20	8.911066	0.096569	0.066691	0.1245	1.2455	0.0085	Fourier
AR1	0.40	8.911066	0.123998	0.093512	0.1246	1.2295	0.0083	Fourier
AR1	0.60	8.911066	0.176484	0.142422	0.1297	1.2172	0.0081	Fourier
Compound symmetry	0.20	8.911066	0.115153	0.070980	0.1298	1.5421	0.0086	Fourier
Compound symmetry	0.40	8.911066	0.135990	0.090871	0.1370	1.6842	0.0085	Fourier
Compound symmetry	0.60	8.911066	0.175110	0.126550	0.1428	2.5201	0.0088	Fourier
Squared Exponential	0.10	8.911066	0.370782	0.334086	0.1482	1.3609	0.0080	Fourier
Squared Exponential	0.15	8.911066	0.710734	0.652240	0.1638	1.4703	0.0084	Fourier
Squared Exponential	0.20	8.911066	0.808248	0.760005	0.1662	1.5090	0.0085	Fourier

Table 10: Effect of proportion of zero values in W . Common settings: conditional distribution of $Y|X(t), Z$: Gaussian distribution (with identity link); smoothed point-wise; sample size: $n = 100$; Covariance function of $U(t)$: squared-exponential with $\rho_u = 0.2$; $\sigma_u = 1$; $q_g = 0$. Benchmark = benchmark method; Average = naïve average method; MM = mixed model based method proposed in Section 2.2; RC = regression calibration method proposed in Section 2.2; Non-ZI MM = non-zero-inflated mixed model based method; 1 day = naive one-day method.

(a) Squared Bias

E(PrW=0)	Benchmark	MM	RC	Average	Non-ZI MM	1 day	basis function
0.255	0.0000903	0.006585	0.007092	0.1074	0.0986	0.3451	Bspline
0.294	0.0000903	0.004534	0.005764	0.1258	0.1323	0.3641	Bspline
0.335	0.0000903	0.003400	0.005045	0.1445	0.1689	0.3822	Bspline
0.403	0.0000903	0.002549	0.003986	0.1770	0.2860	0.4056	Bspline
0.255	0.0128407	0.011672	0.011569	0.1034	0.1074	0.3451	Fourier
0.294	0.0128407	0.011333	0.010548	0.1192	0.1371	0.3641	Fourier
0.335	0.0128407	0.009351	0.009639	0.1378	0.1869	0.3822	Fourier
0.403	0.0128407	0.005167	0.009180	0.1684	0.3403	0.4056	Fourier

(b) Variance

E(PrW=0)	Benchmark	MM	RC	Average	Non-ZI MM	1 day	basis function
0.255	0.001020	0.056708	0.050282	0.0313	0.1827	0.0120	Bspline
0.294	0.001020	0.060766	0.050660	0.0293	0.2373	0.0099	Bspline
0.335	0.001020	0.062859	0.050002	0.0269	0.3297	0.0085	Bspline
0.403	0.001020	0.077295	0.051715	0.0231	0.8235	0.0065	Bspline
0.255	8.911066	1.071181	0.998176	0.1829	0.9043	0.0120	Fourier
0.294	8.911066	0.950327	0.877272	0.1721	1.1069	0.0099	Fourier
0.335	8.911066	0.808248	0.760005	0.1662	1.5090	0.0085	Fourier
0.403	8.911066	0.655488	0.615357	0.1429	3.2846	0.0065	Fourier

Table 11: Effect of q_g for $G(t)$ in Eq (9). Common settings: conditional distribution of $Y|X(t), Z$: Gaussian distribution (with identity link); smoothed point-wise; sample size: $n = 100$; proportion of zero values: $\mathbb{E}\{\Pr(W_{ij}(t) = 0)\} = 0.335$; Covariance function of $U(t)$: squared-exponential with $\rho_u = 0.2$; $\sigma_u = 1$; Benchmark = benchmark method; Average = naïve average method; MM = mixed model based method proposed in Section 2.2; RC = regression calibration method proposed in Section 2.2; Non-ZI MM = non-zero-inflated mixed model based method; 1 day = naive one-day method.

(a) Squared Bias

q_g	Benchmark	MM	RC	Average	Non-ZI MM	1 day	basis function
0.0	0.0000903	0.003400	0.005045	0.1445	0.1689	0.3822	Bspline
0.2	0.0000903	0.001995	0.004874	0.1618	0.0827	0.3818	Bspline
0.4	0.0000903	0.004308	0.004004	0.2052	0.0951	0.3820	Bspline
0.0	0.0128407	0.009351	0.009639	0.1378	0.1869	0.3822	Fourier
0.2	0.0128407	0.011823	0.015466	0.1536	0.0764	0.3818	Fourier
0.4	0.0128407	0.003327	0.008107	0.1970	0.0844	0.3820	Fourier

(b) Variance

q_g	Benchmark	MM	RC	Average	Non-ZI MM	1 day	basis function
0.0	0.001020	0.062859	0.050002	0.0269	0.3297	0.0085	Bspline
0.2	0.001020	0.072695	0.049978	0.0256	0.1898	0.0082	Bspline
0.4	0.001020	0.096320	0.049105	0.0233	0.0789	0.0081	Bspline
0.0	8.911066	0.808248	0.760005	0.1662	1.5090	0.0085	Fourier
0.2	8.911066	0.765011	0.723594	0.1547	0.9039	0.0082	Fourier
0.4	8.911066	0.727050	0.678187	0.1687	0.5337	0.0081	Fourier

Table 12: Effect of sample size. Common settings: Bernoulli distribution (with logit link); estimation method of $\theta(t)$: point-wise; proportion of zero values: $\mathbb{E}\{\Pr(W_{ij}(t) = 0)\} = 0.335$; Covariance function of $U(t)$: squared-exponential with $\rho_u = 0.2$; $\sigma_u = 1$; $q_g = 0$. Benchmark = benchmark method; Average = naïve average method; MM = mixed model based method proposed in Section 2.2; RC = regression calibration method proposed in Section 2.2; Non-ZI MM = non-zero-inflated mixed model based method; 1 day = naive one-day method.

(a) Squared Bias

N	Benchmark	MM	RC	Average	Non-ZI MM	1 day	basis function
50	0.1230072	0.074700	0.064624	0.0758	0.6532	0.3373	Bspline
100	0.0150326	0.049570	0.033648	0.1008	0.2145	0.3878	Bspline
200	0.0119906	0.012999	0.009027	0.1610	0.1734	0.3838	Bspline
500	0.0117602	0.007565	0.006724	0.1439	0.0901	0.3855	Bspline
1000	0.0061865	0.005625	0.009590	0.1508	0.1286	0.3905	Bspline
50	8510.7222608	276.106580	487.760915	0.3125	171.2551	0.3373	Fourier
100	107.4245267	0.546630	0.575267	0.1014	0.5080	0.3878	Fourier
200	21.4239549	0.148504	0.218869	0.1558	0.2650	0.3838	Fourier
500	13.6864192	0.023105	0.051624	0.1375	0.1093	0.3855	Fourier
1000	19.6685291	0.059636	0.053697	0.1404	0.1304	0.3905	Fourier

(b) Variance

N	Benchmark	MM	RC	Average	Non-ZI MM	1 day	basis function
50	4.988905e+01	4.308465e+01	4.164993e+01	6.6078	226.5763	1.0837	Bspline
100	1.430998e+01	1.236682e+01	1.166427e+01	1.9058	20.1516	0.3184	Bspline
200	5.874116e+00	5.087259e+00	5.147803e+00	0.8319	6.0889	0.1413	Bspline
500	2.413604e+00	1.849339e+00	1.890382e+00	0.2662	1.7644	0.0527	Bspline
1000	1.060543e+00	9.195330e-01	9.573540e-01	0.1297	0.8577	0.0248	Bspline
50	4.284808e+06	1.719690e+05	4.035298e+05	73.6180	86927.1378	1.0837	Fourier
100	1.339427e+05	1.957815e+02	1.937196e+02	13.2699	120.6445	0.3184	Fourier
200	5.053468e+04	7.489478e+01	8.055835e+01	5.1519	34.0757	0.1413	Fourier
500	1.651193e+04	2.220087e+01	2.520010e+01	1.6742	10.6785	0.0527	Fourier
1000	7.949001e+03	1.067807e+01	1.254839e+01	0.8060	4.9957	0.0248	Fourier

Table 13: Effect of deviation of U. Common settings: Bernoulli distribution (with logit link); estimation method of $\theta(t)$: point-wise; sample size: $n = 100$; proportion of zero values: $\mathbb{E}\{\Pr(W_{ij}(t) = 0)\} = 0.335$; Covariance function of $U(t)$: squared-exponential with $\rho_u = 0.2$; $q_g = 0$. Benchmark = benchmark method; Average = naïve average method; MM = mixed model based method proposed in Section 2.2; RC = regression calibration method proposed in Section 2.2; Non-ZI MM = non-zero-inflated mixed model based method; 1 day = naive one-day method.

(a) Squared Bias

σ_u	Benchmark	MM	RC	Average	Non-ZI MM	1 day	basis function
1	0.0150326	0.049570	0.033648	0.1008	0.2145	0.3878	Bspline
2	0.0150326	0.111989	0.051939	0.1479	0.1762	0.4200	Bspline
3	0.0150326	0.142549	0.080534	0.2269	569.5784	0.4411	Bspline
1	107.4245267	0.546630	0.575267	0.1014	0.5080	0.3878	Fourier
2	107.4245267	0.384125	0.257744	0.1443	0.8877	0.4200	Fourier
3	107.4245267	0.922071	0.102786	0.2223	14.4792	0.4411	Fourier

(b) Variance

σ_u	Benchmark	MM	RC	Average	Non-ZI MM	1 day	basis function
1	14.30998	12.36682	11.664274	1.9058	20.1516	0.3184	Bspline
2	14.30998	15.11924	8.756273	1.5582	51.9469	0.2542	Bspline
3	14.30998	48.61541	6.456680	1.2733	289780.6263	0.1953	Bspline
1	133942.68329	195.78154	193.719591	13.2699	120.6445	0.3184	Fourier
2	133942.68329	150.64076	87.686845	10.9018	253.1402	0.2542	Fourier
3	133942.68329	491.90707	56.412395	8.6190	17416.4713	0.1953	Fourier

Table 14: Effect of correlation of u . Common settings: Bernoulli distribution (with logit link); estimation method of $\theta(t)$: point-wise; sample size: $n = 100$; proportion of zero values: $\mathbb{E}\{\Pr(W_{ij}(t) = 0)\} = 0.335$; $\sigma_u = 1$; $q_g = 0$. Benchmark = benchmark method; Average = naïve average method; MM = mixed model based method proposed in Section 2.2; RC = regression calibration method proposed in Section 2.2; Non-ZI MM = non-zero-inflated mixed model based method; 1 day = naive one-day method.

(a) Squared Bias

correlation function U	ρ_u	Benchmark	MM	RC	Average	Non-ZI MM	1 day	basis function
AR1	0.20	0.0150326	0.047444	0.040433	0.0961	0.3036	0.3709	Bspline
AR1	0.40	0.0150326	0.052652	0.042118	0.0950	0.3248	0.3748	Bspline
AR1	0.60	0.0150326	0.040998	0.030933	0.0969	0.3013	0.3794	Bspline
Compound symmetry	0.20	0.0150326	0.061152	0.057405	0.0929	0.3586	0.3701	Bspline
Compound symmetry	0.40	0.0150326	0.052440	0.043674	0.0946	0.4973	0.3711	Bspline
Compound symmetry	0.60	0.0150326	0.056921	0.052824	0.0941	0.3707	0.3706	Bspline
Squared Exponential	0.10	0.0150326	0.022937	0.017656	0.1019	0.2524	0.3819	Bspline
Squared Exponential	0.15	0.0150326	0.025354	0.020654	0.1041	0.2693	0.3866	Bspline
Squared Exponential	0.20	0.0150326	0.049570	0.033648	0.1008	0.2145	0.3878	Bspline
AR1	0.20	107.4245267	0.274307	0.250685	0.0974	0.5523	0.3709	Fourier
AR1	0.40	107.4245267	0.150216	0.119055	0.1061	0.5633	0.3748	Fourier
AR1	0.60	107.4245267	0.327863	0.227200	0.1079	0.5313	0.3794	Fourier
Compound symmetry	0.20	107.4245267	0.210395	0.172365	0.0935	0.6425	0.3701	Fourier
Compound symmetry	0.40	107.4245267	0.165175	0.182104	0.0905	0.6127	0.3711	Fourier
Compound symmetry	0.60	107.4245267	0.147165	0.116096	0.0916	0.6691	0.3706	Fourier
Squared Exponential	0.10	107.4245267	0.379175	0.379208	0.1065	0.5471	0.3819	Fourier
Squared Exponential	0.15	107.4245267	0.261578	0.389972	0.1134	0.5281	0.3866	Fourier
Squared Exponential	0.20	107.4245267	0.546630	0.575267	0.1014	0.5080	0.3878	Fourier

(b) Variance

correlation function U	ρ_u	Benchmark	MM	RC	Average	Non-ZI MM	1 day	basis function
AR1	0.20	14.30998	9.189825	8.914817	1.9079	19.1846	0.3298	Bspline
AR1	0.40	14.30998	9.564324	9.233625	1.8525	18.1525	0.3209	Bspline
AR1	0.60	14.30998	9.923213	9.475688	1.8980	18.8789	0.3144	Bspline
Compound symmetry	0.20	14.30998	10.899403	10.620337	1.9477	18.3008	0.3291	Bspline
Compound symmetry	0.40	14.30998	10.895815	10.663124	1.8911	38.9483	0.3287	Bspline
Compound symmetry	0.60	14.30998	11.548294	11.015541	1.9159	18.2469	0.3316	Bspline
Squared Exponential	0.10	14.30998	8.560971	8.125550	1.8312	18.2983	0.3055	Bspline
Squared Exponential	0.15	14.30998	11.100982	10.645155	1.8191	18.4807	0.3106	Bspline
Squared Exponential	0.20	14.30998	12.366820	11.664274	1.9058	20.1516	0.3184	Bspline
AR1	0.20	133942.68329	60.189778	58.157740	11.0185	94.0496	0.3298	Fourier
AR1	0.40	133942.68329	62.434690	59.305086	10.8672	101.7753	0.3209	Fourier
AR1	0.60	133942.68329	73.484362	70.415540	11.7778	119.6064	0.3144	Fourier
Compound symmetry	0.20	133942.68329	78.125086	75.306457	11.5590	95.3529	0.3291	Fourier
Compound symmetry	0.40	133942.68329	87.018630	84.761023	11.8844	103.7438	0.3287	Fourier
Compound symmetry	0.60	133942.68329	104.651268	102.823516	12.6293	108.1200	0.3316	Fourier
Squared Exponential	0.10	133942.68329	119.483667	120.043084	12.1252	114.2930	0.3055	Fourier
Squared Exponential	0.15	133942.68329	175.507967	174.291604	13.0771	115.7622	0.3106	Fourier
Squared Exponential	0.20	133942.68329	195.781545	193.719591	13.2699	120.6445	0.3184	Fourier

Table 15: Effect of proportion of zero values in W . Common settings: Bernoulli distribution (with logit link); estimation method of $\theta(t)$: point-wise; sample size: $n = 100$; Covariance function of $U(t)$: squared-exponential with $\rho_u = 0.2$; $\sigma_u = 1$; $q_g = 0$. Benchmark = benchmark method; Average = naïve average method; MM = mixed model based method proposed in Section 2.2; RC = regression calibration method proposed in Section 2.2; Non-ZI MM = non-zero-inflated mixed model based method; 1 day = naive one-day method.

(a) Squared Bias							
E(PrW=0)	Benchmark	MM	RC	Average	Non-ZI MM	1 day	basis function
0.255	0.0150326	0.050779	0.039638	0.0645	0.1668	0.3503	Bspline
0.294	0.0150326	0.040168	0.028547	0.0772	0.1833	0.3699	Bspline
0.335	0.0150326	0.049570	0.033648	0.1008	0.2145	0.3878	Bspline
0.403	0.0150326	0.060177	0.036469	0.1329	0.2759	0.4077	Bspline
0.255	107.4245267	1.280489	0.903613	0.0807	0.3221	0.3503	Fourier
0.294	107.4245267	0.442614	0.523684	0.0904	0.4478	0.3699	Fourier
0.335	107.4245267	0.546630	0.575267	0.1014	0.5080	0.3878	Fourier
0.403	107.4245267	0.230456	0.635797	0.1276	1.0988	0.4077	Fourier

(b) Variance							
E(PrW=0)	Benchmark	MM	RC	Average	Non-ZI MM	1 day	basis function
0.255	14.30998	13.33442	12.76470	2.5310	13.1404	0.4871	Bspline
0.294	14.30998	12.83989	12.33306	2.2693	16.4019	0.3980	Bspline
0.335	14.30998	12.36682	11.66427	1.9058	20.1516	0.3184	Bspline
0.403	14.30998	10.72348	10.80394	1.5109	53.4614	0.2436	Bspline
0.255	133942.68329	279.38631	261.94404	19.6025	95.7604	0.4871	Fourier
0.294	133942.68329	238.04848	223.39025	15.8953	105.0335	0.3980	Fourier
0.335	133942.68329	195.78154	193.71959	13.2699	120.6445	0.3184	Fourier
0.403	133942.68329	132.47330	156.03496	9.8360	191.8466	0.2436	Fourier

Table 16: Effect of q_g for $G(t)$ in Eq (9). Common settings: Bernoulli distribution (with logit link); estimation method of $\theta(t)$: point-wise; sample size: $n = 100$; proportion of zero values: $\mathbb{E}\{\Pr(W_{ij}(t) = 0)\} = 0.335$; Covariance function of $U(t)$: squared-exponential with $\rho_u = 0.2$; $\sigma_u = 1$; Benchmark = benchmark method; Average = naïve average method; MM = mixed model based method proposed in Section 2.2; RC = regression calibration method proposed in Section 2.2; Non-ZI MM = non-zero-inflated mixed model based method; 1 day = naive one-day method.

(a) Squared Bias							
q_g	Benchmark	MM	RC	Average	Non-ZI MM	1 day	basis function
0.0	0.0150326	0.049570	0.033648	0.1008	0.2145	0.3878	Bspline
0.2	0.0150326	0.044423	0.033209	0.1330	0.1476	0.3887	Bspline
0.4	0.0150326	0.022480	0.031240	0.1829	0.1060	0.3876	Bspline
0.0	107.4245267	0.546630	0.575267	0.1014	0.5080	0.3878	Fourier
0.2	107.4245267	0.344596	0.517744	0.1545	0.4463	0.3887	Fourier
0.4	107.4245267	0.215212	0.468406	0.1729	0.1486	0.3876	Fourier

(b) Variance							
q_g	Benchmark	MM	RC	Average	Non-ZI MM	1 day	basis function
0.0	14.30998	12.366820	11.66427	1.9058	20.1516	0.3184	Bspline
0.2	14.30998	11.833070	11.60735	1.6796	10.8239	0.3191	Bspline
0.4	14.30998	8.546491	11.00679	1.2983	4.2749	0.3277	Bspline
0.0	133942.68329	195.781545	193.71959	13.2699	120.6445	0.3184	Fourier
0.2	133942.68329	182.521904	189.75403	13.0345	76.2574	0.3191	Fourier
0.4	133942.68329	117.085774	163.64099	10.4905	33.8754	0.3277	Fourier

Table 17: Effect of sample size. Common settings: Bernoulli distribution (with logit link); smoothed point-wise; proportion of zero values: $\mathbb{E}\{\Pr(W_{ij}(t) = 0)\} = 0.335$; Covariance function of $U(t)$: squared-exponential with $\rho_u = 0.2$; $\sigma_u = 1$; $q_g = 0$. Benchmark = benchmark method; Average = naïve average method; MM = mixed model based method proposed in Section 2.2; RC = regression calibration method proposed in Section 2.2; Non-ZI MM = non-zero-inflated mixed model based method; 1 day = naive one-day method.

(a) Squared Bias							
N	Benchmark	MM	RC	Average	Non-ZI MM	1 day	basis function
50	0.1230072	0.073128	0.063324	0.0758	0.6532	0.3373	Bspline
100	0.0150326	0.050386	0.035714	0.1008	0.2145	0.3878	Bspline
200	0.0119906	0.012468	0.008708	0.1610	0.1734	0.3838	Bspline
500	0.0117602	0.007298	0.006896	0.1439	0.0901	0.3855	Bspline
1000	0.0061865	0.005265	0.009536	0.1508	0.1286	0.3905	Bspline
50	8510.7222608	11307.977149	3.445035	0.3125	171.2551	0.3373	Fourier
100	107.4245267	0.508382	0.433005	0.1014	0.5080	0.3878	Fourier
200	21.4239549	0.151802	0.197691	0.1558	0.2650	0.3838	Fourier
500	13.6864192	0.021474	0.053488	0.1375	0.1093	0.3855	Fourier
1000	19.6685291	0.057265	0.051438	0.1404	0.1304	0.3905	Fourier

(b) Variance							
N	Benchmark	MM	RC	Average	Non-ZI MM	1 day	basis function
50	4.988905e+01	4.299165e+01	41.845801	6.6078	226.5763	1.0837	Bspline
100	1.430998e+01	1.230884e+01	11.617732	1.9058	20.1516	0.3184	Bspline
200	5.874116e+00	5.085867e+00	5.139273	0.8319	6.0889	0.1413	Bspline
500	2.413604e+00	1.836943e+00	1.880630	0.2662	1.7644	0.0527	Bspline
1000	1.060543e+00	9.194920e-01	0.956270	0.1297	0.8577	0.0248	Bspline
50	4.284808e+06	5.636157e+06	1428.345493	73.6180	86927.1378	1.0837	Fourier
100	1.339427e+05	1.990476e+02	195.187175	13.2699	120.6445	0.3184	Fourier
200	5.053468e+04	7.541321e+01	80.556140	5.1519	34.0757	0.1413	Fourier
500	1.651193e+04	2.225222e+01	25.129643	1.6742	10.6785	0.0527	Fourier
1000	7.949001e+03	1.057006e+01	12.464185	0.8060	4.9957	0.0248	Fourier

Table 18: Effect of deviation of U. Common settings: Bernoulli distribution (with logit link); smoothed point-wise; sample size: $n = 100$; proportion of zero values: $\mathbb{E}\{\Pr(W_{ij}(t) = 0)\} = 0.335$; Covariance function of $U(t)$: squared-exponential with $\rho_u = 0.2$; $q_g = 0$. Benchmark = benchmark method; Average = naïve average method; MM = mixed model based method proposed in Section 2.2; RC = regression calibration method proposed in Section 2.2; Non-ZI MM = non-zero-inflated mixed model based method; 1 day = naive one-day method.

(a) Squared Bias							
σ_u	Benchmark	MM	RC	Average	Non-ZI MM	1 day	basis function
1	0.0150326	0.050386	0.035714	0.1008	0.2145	0.3878	Bspline
2	0.0150326	0.114038	0.052613	0.1479	0.1762	0.4200	Bspline
3	0.0150326	0.149900	0.081176	0.2269	569.5784	0.4411	Bspline
1	107.4245267	0.508382	0.433005	0.1014	0.5080	0.3878	Fourier
2	107.4245267	0.384697	0.239458	0.1443	0.8877	0.4200	Fourier
3	107.4245267	0.953764	0.102823	0.2223	14.4792	0.4411	Fourier

(b) Variance							
σ_u	Benchmark	MM	RC	Average	Non-ZI MM	1 day	basis function
1	14.30998	12.30884	11.617732	1.9058	20.1516	0.3184	Bspline
2	14.30998	15.06918	8.722044	1.5582	51.9469	0.2542	Bspline
3	14.30998	45.31736	6.450979	1.2733	289780.6263	0.1953	Bspline
1	133942.68329	199.04763	195.187175	13.2699	120.6445	0.3184	Fourier
2	133942.68329	152.37204	87.743007	10.9018	253.1402	0.2542	Fourier
3	133942.68329	515.57976	56.601526	8.6190	17416.4713	0.1953	Fourier

Table 19: Effect of correlation of u . Common settings: Bernoulli distribution (with logit link); smoothed point-wise; sample size: $n = 100$; proportion of zero values: $\mathbb{E}\{\Pr(W_{ij}(t) = 0)\} = 0.335$; $\sigma_u = 1$; $q_g = 0$. Benchmark = benchmark method; Average = naïve average method; MM = mixed model based method proposed in Section 2.2; RC = regression calibration method proposed in Section 2.2; Non-ZI MM = non-zero-inflated mixed model based method; 1 day = naive one-day method.

(a) Squared Bias

correlation function U	ρ_u	Benchmark	MM	RC	Average	Non-ZI MM	1 day	basis function
AR1	0.20	0.0150326	0.047030	0.039978	0.0961	0.3036	0.3709	Bspline
AR1	0.40	0.0150326	0.053365	0.043068	0.0950	0.3248	0.3748	Bspline
AR1	0.60	0.0150326	0.041493	0.031321	0.0969	0.3013	0.3794	Bspline
Compound symmetry	0.20	0.0150326	0.061318	0.058211	0.0929	0.3586	0.3701	Bspline
Compound symmetry	0.40	0.0150326	0.052949	0.044449	0.0946	0.4973	0.3711	Bspline
Compound symmetry	0.60	0.0150326	0.056266	0.052737	0.0941	0.3707	0.3706	Bspline
Squared Exponential	0.10	0.0150326	0.022744	0.017715	0.1019	0.2524	0.3819	Bspline
Squared Exponential	0.15	0.0150326	0.025846	0.019917	0.1041	0.2693	0.3866	Bspline
Squared Exponential	0.20	0.0150326	0.050386	0.035714	0.1008	0.2145	0.3878	Bspline
AR1	0.20	107.4245267	0.283537	0.259335	0.0974	0.5523	0.3709	Fourier
AR1	0.40	107.4245267	0.153780	0.121301	0.1061	0.5633	0.3748	Fourier
AR1	0.60	107.4245267	0.348051	0.231356	0.1079	0.5313	0.3794	Fourier
Compound symmetry	0.20	107.4245267	0.222522	0.181032	0.0935	0.6425	0.3701	Fourier
Compound symmetry	0.40	107.4245267	0.162984	0.185270	0.0905	0.6127	0.3711	Fourier
Compound symmetry	0.60	107.4245267	0.144948	0.115386	0.0916	0.6691	0.3706	Fourier
Squared Exponential	0.10	107.4245267	0.389426	0.413785	0.1065	0.5471	0.3819	Fourier
Squared Exponential	0.15	107.4245267	0.240888	0.304061	0.1134	0.5281	0.3866	Fourier
Squared Exponential	0.20	107.4245267	0.508382	0.433005	0.1014	0.5080	0.3878	Fourier

(b) Variance

correlation function U	ρ_u	Benchmark	MM	RC	Average	Non-ZI MM	1 day	basis function
AR1	0.20	14.30998	9.189542	8.901574	1.9079	19.1846	0.3298	Bspline
AR1	0.40	14.30998	9.560459	9.215958	1.8525	18.1525	0.3209	Bspline
AR1	0.60	14.30998	9.900726	9.480119	1.8980	18.8789	0.3144	Bspline
Compound symmetry	0.20	14.30998	10.840769	10.624313	1.9477	18.3008	0.3291	Bspline
Compound symmetry	0.40	14.30998	10.940169	10.729000	1.8911	38.9483	0.3287	Bspline
Compound symmetry	0.60	14.30998	11.512976	11.052571	1.9159	18.2469	0.3316	Bspline
Squared Exponential	0.10	14.30998	8.566455	8.126454	1.8312	18.2983	0.3055	Bspline
Squared Exponential	0.15	14.30998	11.061876	10.623938	1.8191	18.4807	0.3106	Bspline
Squared Exponential	0.20	14.30998	12.308843	11.617732	1.9058	20.1516	0.3184	Bspline
AR1	0.20	133942.68329	60.612574	58.359882	11.0185	94.0496	0.3298	Fourier
AR1	0.40	133942.68329	62.163259	58.847516	10.8672	101.7753	0.3209	Fourier
AR1	0.60	133942.68329	73.174854	70.377144	11.7778	119.6064	0.3144	Fourier
Compound symmetry	0.20	133942.68329	78.419842	75.447020	11.5590	95.3529	0.3291	Fourier
Compound symmetry	0.40	133942.68329	87.418195	85.217615	11.8844	103.7438	0.3287	Fourier
Compound symmetry	0.60	133942.68329	105.645114	103.465558	12.6293	108.1200	0.3316	Fourier
Squared Exponential	0.10	133942.68329	120.781684	121.525296	12.1252	114.2930	0.3055	Fourier
Squared Exponential	0.15	133942.68329	178.018432	175.560460	13.0771	115.7622	0.3106	Fourier
Squared Exponential	0.20	133942.68329	199.047625	195.187175	13.2699	120.6445	0.3184	Fourier

Table 20: Effect of proportion of zero values in W . Common settings: Bernoulli distribution (with logit link); smoothed point-wise; sample size: $n = 100$; Covariance function of $U(t)$: squared-exponential with $\rho_u = 0.2$; $\sigma_u = 1$; $q_g = 0$. Benchmark = benchmark method; Average = naïve average method; MM = mixed model based method proposed in Section 2.2; RC = regression calibration method proposed in Section 2.2; Non-ZI MM = non-zero-inflated mixed model based method; 1 day = naive one-day method.

(a) Squared Bias							
E(PrW=0)	Benchmark	MM	RC	Average	Non-ZI MM	1 day	basis function
0.255	0.0150326	0.051167	0.040753	0.0645	0.1668	0.3503	Bspline
0.294	0.0150326	0.041507	0.030263	0.0772	0.1833	0.3699	Bspline
0.335	0.0150326	0.050386	0.035714	0.1008	0.2145	0.3878	Bspline
0.403	0.0150326	0.060706	0.038519	0.1329	0.2759	0.4077	Bspline
0.255	107.4245267	1.280440	0.935615	0.0807	0.3221	0.3503	Fourier
0.294	107.4245267	0.399134	0.396307	0.0904	0.4478	0.3699	Fourier
0.335	107.4245267	0.508382	0.433005	0.1014	0.5080	0.3878	Fourier
0.403	107.4245267	0.248041	0.628551	0.1276	1.0988	0.4077	Fourier

(b) Variance							
E(PrW=0)	Benchmark	MM	RC	Average	Non-ZI MM	1 day	basis function
0.255	14.30998	13.32331	12.73832	2.5310	13.1404	0.4871	Bspline
0.294	14.30998	12.81114	12.29866	2.2693	16.4019	0.3980	Bspline
0.335	14.30998	12.30884	11.61773	1.9058	20.1516	0.3184	Bspline
0.403	14.30998	10.66842	10.74905	1.5109	53.4614	0.2436	Bspline
0.255	133942.68329	283.62098	265.61055	19.6025	95.7604	0.4871	Fourier
0.294	133942.68329	239.78025	224.45952	15.8953	105.0335	0.3980	Fourier
0.335	133942.68329	199.04763	195.18717	13.2699	120.6445	0.3184	Fourier
0.403	133942.68329	134.04625	155.68044	9.8360	191.8466	0.2436	Fourier

Table 21: Effect of q_g for $G(t)$ in Eq (9). Common settings: Bernoulli distribution (with logit link); smoothed point-wise; sample size: $n = 100$; proportion of zero values: $\mathbb{E}\{\Pr(W_{ij}(t) = 0)\} = 0.335$; Covariance function of $U(t)$: squared-exponential with $\rho_u = 0.2$; $\sigma_u = 1$; Benchmark = benchmark method; Average = naïve average method; MM = mixed model based method proposed in Section 2.2; RC = regression calibration method proposed in Section 2.2; Non-ZI MM = non-zero-inflated mixed model based method; 1 day = naive one-day method.

(a) Squared Bias							
q_g	Benchmark	MM	RC	Average	Non-ZI MM	1 day	basis function
0.0	0.0150326	0.050386	0.035714	0.1008	0.2145	0.3878	Bspline
0.2	0.0150326	0.045836	0.035390	0.1330	0.1476	0.3887	Bspline
0.4	0.0150326	0.023270	0.032864	0.1829	0.1060	0.3876	Bspline
0.0	107.4245267	0.508382	0.433005	0.1014	0.5080	0.3878	Fourier
0.2	107.4245267	0.359648	0.440845	0.1545	0.4463	0.3887	Fourier
0.4	107.4245267	0.206262	0.453843	0.1729	0.1486	0.3876	Fourier

(b) Variance							
q_g	Benchmark	MM	RC	Average	Non-ZI MM	1 day	basis function
0.0	14.30998	12.308843	11.61773	1.9058	20.1516	0.3184	Bspline
0.2	14.30998	11.778162	11.59655	1.6796	10.8239	0.3191	Bspline
0.4	14.30998	8.521128	10.96912	1.2983	4.2749	0.3277	Bspline
0.0	133942.68329	199.047625	195.18717	13.2699	120.6445	0.3184	Fourier
0.2	133942.68329	188.240261	191.84586	13.0345	76.2574	0.3191	Fourier
0.4	133942.68329	119.301798	166.51689	10.4905	33.8754	0.3277	Fourier